

PERFORMANCE EVALUATION OF MULTI-HOP WPANS BASED ON A
REALISTIC OFDM UWB PHYSICAL LAYER

by

HONGJU GAO

A Dissertation submitted to the
Graduate School-New Brunswick
Rutgers, The State University of New Jersey
in partial fulfillment of the requirements

for the degree of

Doctor of Philosophy

Graduate Program in

Electrical and Computer Engineering

written under the direction of

Professor David G. Daut

and approved by

New Brunswick, New Jersey

October, 2007

ABSTRACT OF THE DISSERTATION

Performance Evaluation of Multi-Hop WPANs Based on a Realistic OFDM UWB

Physical Layer

by Hongju Gao

Dissertation Director:

Professor David G. Daut

MB-OFDM (Multi-Band Orthogonal Frequency Division Multiplexing) is one of the promising candidates for the UWB (Ultra-Wide-Band)-based alternative physical (PHY) layer for WPANs (Wireless Personal Area Networks). However, the coverage radius of MB-OFDM UWB systems is very short, and single-hop transmissions may not be adequate for WPANs operating at very high-data-rates. Therefore, a multi-hop ad hoc WPAN system is considered in this study in order to extend the UWB radio coverage. The overall system performance is obtained to determine if the Quality-of-Service parameters can still be preserved when an IEEE 802.15.3 TDMA MAC layer is used in multi-hop communication scenarios.

A position-based stateless routing protocol with greedy forwarding is adopted in this study for multi-hop WPANs. Simulation results show that the position-based stateless greedy routing scheme with carefully selected transmission radius R meets the QoS performance criteria for many real-time applications before saturation of the network

occurs. Hence, the scheme is a good choice for the routing protocol to be used with multi-hop WPANs based on an OFDM UWB physical layer.

At the MAC layer, when using equal-weighted topology-based scheduling, it can be observed that the system performance obtained can meet QoS requirements only when either the data rate is very low, or there are only a very small number of active links. Network capacities actually achieved for both 200 and 480 Mbps transmission systems are much less than those predicted by theory since the network bandwidth is not utilized efficiently. When using the on-demand rate-based scheduling scheme, the performance results for both the 200 and 480 Mbps transmission systems match the network capacity levels expected for multi-hop WPANs. The scheduling efficiency is comparatively high for the on-demand scheduling scheme, and hence, network bandwidth can be utilized more efficiently. It has been found that the IEEE 802.15.3 TDMA MAC layer, with the proper scheduling and routing schemes can satisfactorily meet QoS requirements in the context of multi-hop networks. Multi-hop WPAN based on the OFDM UWB physical layer has been determined to be a viable approach to extend the network coverage while adequately supporting very high data rate multimedia traffic.

Acknowledgements

Firstly, I would like to thank Professor David G. Daut for his supervision, for his assistance, guidance, support and patience during the course of this research effort. I have enjoyed and benefited very much from working under his supervision.

I also would like to thank Professor Ivan Marsic, Professor Wade Trappe, Professor Yanyong Zhang, and Dr. Jaewon Kang for taking time from their busy schedules to serve on my dissertation committee. Their valuable comments and suggestions have greatly aided the completion of this study.

Finally, I would like to thank Angela Xa and John Scafidi of the ECE Computer Laboratory for setting up and maintaining the software used in the conduct of this thesis research.

Table of Contents

ABSTRACT OF THE DISSERTATION	ii
Acknowledgements	iv
Table of Contents	v
List of Tables	viii
List of Figures	ix
Chapter 1 Introduction	1
1.1 Overview of a Wireless Personal Area Network (WPAN).....	2
1.2 UWB Physical Layer	5
1.3 Multi-Hop Ad Hoc WPAN System	7
1.4 Challenges Present in Multi-Hop Networks	10
1.5 Outline of the Dissertation	13
Chapter 2 OFDM UWB Physical Layer	15
2.1 Ultra-Wide-Band (UWB) Radio Communications.....	15
2.1.1 Definition of UWB	16
2.1.2 UWB Radio Signals.....	19
2.2 MBOA Multi-Band OFDM Physical Layer Proposal	20
2.2.1 Mathematical Description of the OFDM Signal.....	22
2.2.2 OFDM Modulation and Parameters.....	23
2.2.3 Transmission Modes and Access Schemes.....	26
2.2.4 Receiver Sensitivity	27
2.3 Performance of the MBOA OFDM UWB Physical Layer	27

2.4	Coverage Radius of the MBOA OFDM System.....	29
2.5	Physical Layer Implementation Using Qualnet	30
Chapter 3 WPAN MAC Layer.....		32
3.1	MAC Layer Protocol.....	32
3.2	IEEE 802.15.3 MAC Layer	33
3.3	Basics of Time Division Multiple Access (TDMA).....	36
3.4	Scheduling in TDMA.....	37
3.5	Implementation of the TDMA MAC Layer Using Qualnet.....	38
Chapter 4 WPAN System Description.....		39
4.1	Description of the Overall System.....	39
4.2	Quality-of-Service Requirements	43
4.3	System Performance Criteria	43
4.4	Network Capacity of a Single-Hop WPAN	46
4.5	Capacity Analysis of a Multi-Hop Network	49
Chapter 5 Simulation Results for Single-Hop WPAN Systems		51
5.1	4m × 4m Single-Hop System.....	53
5.2	10m x 10m Single-Hop System	56
5.3	Conclusions for Single-Hop Scenarios	59
Chapter 6 Routing Protocols Based on a Realistic Physical Layer		60
6.1	Issues in Designing a Routing Protocol	61

6.2	Existing Routing Protocols	62
6.3	Routing Protocols Based on a Realistic Physical Layer	64
6.4	Position-Based Greedy Stateless Routing.....	68
6.5	Simulation Results	71
6.5.1	Simulation Results for Transmission Systems Operating at 200 Mbps....	72
6.5.2	Simulation Results for Transmission Systems Operating at 480 Mbps....	75
6.5.3	Conclusions.....	77
Chapter 7 Simulation Results for Multi-Hop WPAN Systems.....		79
7.1	System Parameters for Multi-Hop Scenarios.....	79
7.2	Simulation Results for Equal-Weighted Node-Based Scheduling.....	82
7.3	Simulation Results for On-Demand Link-Based Scheduling	87
7.4	Conclusions.....	91
Chapter 8 Conclusions and Future Work.....		92
8.1	Contributions of the Thesis.....	92
8.2	Future Work.....	95
References.....		97
Curriculum Vitae		100

List of Tables

Table 2.1: Rate-Dependent Parameters for the MBOA OFDM UWB Physical Layer. ..	22
Table 2.2: Timing-Related Parameters for the MBOA OFDM UWB Physical Layer....	25
Table 2.3: Band Allocation for the MBOA OFDM UWB Physical Layer.....	26
Table 2.4: Receiver Performance Requirements for the MBOA OFDM UWB Physical Layer.....	27
Table 2.5: Range to Achieve a PER of 8% With a 90% Link Success Probability for Mode 1 Devices [11].	30
Table 4.1: QoS Requirements for Different Applications.	43
Table 4.2: Throughput for a 1024 Byte Packet vs. Data Rate (single/multiple frames)..	48
Table 5.1: Simulation Parameters and Values for Single-Hop Scenarios.	52
Table 6.1: Parameters and Values Used in System Simulations.	72
Table 6.2: Average Hop Count for Transmission Systems Operating at 200 Mbps.....	75
Table 6.3: Average Hop Count for Transmission Systems Operating at 480 Mbps.....	77
Table 7.1: Simulation Parameters and Values for Multi-Hop Network Scenarios.....	82

List of Figures

Figure 2.1: Spectrum of UWB Systems Compared With IEEE 802.11b and 802.11a...	18
Figure 2.2: Frequency of Operation for a Mode 1 Device.....	27
Figure 2.3: MBOA OFDM Transmitter [10].	28
Figure 2.4: BER Performance vs. Ebu/No for CM1 Channel.....	29
Figure 3.1: Superframe Structure in an IEEE 802.15.3 Piconet.	34
Figure 4.1: Total Throughput vs. Packet Generation Rate Per Link.	48
Figure 5.1: Average End-to-End Delay vs. Number of Source-Destination Pairs for Single-Hop Scenario: 4m x 4m Area.....	55
Figure 5.2: PFR vs. Number of Source-Destination Pairs for the Single-Hop Scenario: 4m x 4m Area.	55
Figure 5.3: Throughput vs. Number of Source-Destination Pairs for Single-Hop Scenario: 4m x 4m Area.	56
Figure 5.4: Average End-to-End Delay vs. Number of Source-Destination Pairs for Single-Hop Scenario: 10m x 10m Area.....	58
Figure 5.5: PFR vs. Number of Source-Destination Pairs for Single-Hop Scenario: 10m x 10m Area.	58
Figure 5.6: Throughput vs. Number of Source-Destination Pairs for Single-Hop Scenario: 10m x 10m Area.	59
Figure 6.1: Packet Reception Probability as a Function of Distance in a Typical Physical Layer Model [16].	65
Figure 6.2: PER vs. Distance for the Proposed OFDM UWB Physical Layer [6].	66

Figure 6.3: Illustration of Position-Based Routing [17].	71
Figure 6.4: Average Delay vs. Number of Source-Destination Pairs With R as a Parameter for Transmission Systems Operating at 200 Mbps.	74
Figure 6.5: PFR vs. Number of Source-Destination Pairs With R as a Parameter for Transmission Systems Operating at 200 Mbps.	74
Figure 6.6: Average Delay vs. Number of Source-Destination Pairs with R as a Parameter for Transmission Systems Operating at 480 Mbps.	76
Figure 6.7: PFR vs. Number of Source-Destination Pairs with R as a Parameter for Transmission Systems Operating at 480 Mbps.	77
Figure 7.1: Average Delay vs. Number of Source-Destination Pairs With Equal- Weighted Scheduling for Transmission Systems Operating at 200 Mbps. ..	85
Figure 7.2: PFR vs. Number of Source-Destination Pairs With Equal-Weighted Scheduling for Transmission Systems Operating at 200 Mbps.....	85
Figure 7.3: Average Delay vs. Number of Source-Destination Pairs With Equal- Weighted Scheduling for Transmission Systems Operating at 480 Mbps. ..	86
Figure 7.4: PFR vs. Number of Source-Destination Pairs With Equal-Weighted Scheduling for Transmission Systems Operating at 480 Mbps.....	86
Figure 7.5: Average Delay vs. Number of Source-Destination Pairs With On-Demand Scheduling for Transmission Systems Operating at 200 Mbps.....	89
Figure 7.6: PFR vs. Number of Source-Destination Pairs With On-Demand Scheduling for Transmission Systems Operating at 200 Mbps.....	89
Figure 7.7: Average Delay vs. Number of Source-Destination Pairs With On-Demand Scheduling for Transmission Systems Operating at 480 Mbps.....	90

Figure 7.8: PFR vs. Number of Source-Destination Pairs With On-Demand Scheduling
for Transmission Systems Operating at 480 Mbps..... 90

Chapter 1

Introduction

Recent advances in consumer electronics (camcorders, DVD players, etc) have created a great need for wireless communications systems that operate at very high data rates over short distances. The high-rate Wireless Personal Area Network (WPAN), which enables short-range ad hoc connectivity among consumer electronics and communications devices, has attracted increasing interest in both academia and industry since 2000. The approval by the Federal Communications Commission (FCC) for the use of Ultra-Wide-Band (UWB) on the unlicensed band in the 3.1-10.6 GHz range in 2002 has led to considerable interest in exploiting very high-rate WPAN systems (up to 480 Mbps) based on a UWB physical layer implementation. However, the coverage radius of a UWB system is very short, and peer-to-peer communication may be not sufficient to support very high-data-rate transmission. Therefore, multi-hop ad hoc WPAN is being considered to extend the UWB radio coverage. Since the IEEE 802.15.3 Standard is designed for peer-to-peer communication, the following question arises: can an acceptable level of Quality-of-Service still be preserved in multi-hop scenarios? In this study, thorough and complete investigations using simulation have been conducted. Performance results are presented to provide quantitative answers to this important question.

In this chapter, an overview of a Wireless Personal Area Network is first given, then UWB radio communications fundamentals are introduced, and finally the concept of

multi-hop WPAN is briefly presented. The challenges present in multi-hop ad hoc WPAN systems are discussed. In the last section, an outline of the overall dissertation research effort is presented.

1.1 Overview of a Wireless Personal Area Network (WPAN)

Wireless Personal Area Networks (WPANs) enable short-range ad hoc connectivity among portable consumer electronics and communications devices. The coverage area for a WPAN is generally within a 10 meter radius [1]. The Bluetooth radio system has emerged as the first technology addressing WPAN applications with its prominent features of low power consumption, small package size, and low cost [1]. Data rates for Bluetooth devices are limited to 1 Mbps for version 1.2, and 3 Mbps for version 2.0 with enhanced data rate (EDR), respectively. These data rates are enough for streaming stereo audio, transferring data or carrying voice communications, but they are not enough to support multimedia traffic. The IEEE 802.15.1 Standard was derived from the Bluetooth version 1.1 Foundation Specifications, and was published in June 2002.

The next generation of portable consumer electronics and communications devices will support multimedia data traffic that inherently require high data rates. Applications include high-quality video and audio distribution, and multi-megabyte file transfers for music and image files [1]. Example devices that will use high-rate WPANs include digital camcorders, digital televisions, digital cameras, MP3 players, printers, projectors, and laptops, etc [1]. The need for communications between these multimedia-capable devices leads to peer-to-peer ad hoc type connections that warrant data rates well in

excess of 20 Mbps and Quality of Service (QoS) provisions with respect to guaranteed bandwidth [1].

To accommodate the required physical layer and MAC layer QoS requirements, the IEEE 802.15 WPAN Working Group initiated a new group, the 802.15.3 High-Rate WPAN Task Group. The IEEE 802.15.3 Standard was designed to enable wireless connectivity of high-speed, low-power, low-cost, multimedia-capable consumer electronic devices [26]. The idea of adding high-rate capability to the IEEE 802.15 family of standards was first proposed in November 1999. The 802.15.3 Task Group began their official work in March 2000, and 802.15.3 was finally approved as an IEEE Standard in June 2003. This Standard is not intended to be a simple extension of the IEEE 802.15.1 Standard because the MAC needs are very different [26].

Generally, an IEEE 802.15.3 compliant WPAN operates in the unlicensed 2.4 GHz frequency band with an RF bandwidth of 15 MHz. The symbol rate is 11 Mbps and applies to all specified modulation formats, including QPSK, DQPSK, and 16/32/64 QAM [1]. The achievable data rates can be in the range from 11 Mbps to 55 Mbps through the use of multi-bit symbol modulation and channel coding.

For applications that involve imaging and multimedia, such as H.323/T.120 video conferences, home theater, interactive applications, and file downloading, a much higher data rate is required than that specified in the IEEE 805.15.3 Standard. The IEEE 802.15 High Rate Alternative PHY Task Group (TG3a) for WPANs was established to define a

project to provide a higher speed PHY enhancement amendment to 802.15.3 for these applications. This alternative physical layer (alt-PHY) is intended as a supplement to the IEEE 802.15.3 Standard.

A bit rate of at least 110 Mb/s at a distance of 10 meters is required to be supported by the physical layer. The transmit power is fixed by regulatory emission limits. An additional higher bit rate of at least 200 Mb/s at a distance of 4 meters is required. Scalability to rates in excess of 480 Mb/s is desirable even at the expense of reduced operating distances. The data rates mentioned above are minimums and data rates in the actual proposals may be higher. Most proposals favor the Ultra Wide Band physical layer implementation approach to realize the desired system specifications.

Wireless personal area networks (WPANs) are used to convey information over relatively short distances among a few participants [26]. A WPAN is distinguished from other types of data networks in that communications are normally confined to a small area that typically covers about 10 meters in radius and completely envelops connected equipment whether stationary or in motion. High-Rate WPAN enables multimedia connectivity between portable devices within a Personal Operating Space (POS). A set of devices within a POS, which operate under the control of a piconet controller (PNC) in order to share a wireless resource, is called a piconet. The function of the PNC is to provide the basic timing for the WPAN. Additionally, the PNC manages the Quality-of-Service (QoS) requirements for the WPAN as a whole.

The main characteristics of a WPAN are as follows:

- **High Rate.** WPAN operates within a short range at a high data rate. A range of at least 10 m, and up to 70 m is possible. Currently, the data rate realized is 55 Mb/s. The rate is to be increased up to 100-400 Mb/s by the use of an alternative physical layer implementation.
- **Dynamic Topology.** Mobile devices often join and leave a piconet while requiring only a short time to connect to the network ($< 1s$).
- **Ad-hoc Network with Multimedia QoS Provisions.** IEEE 802.15.3 WPAN uses TDMA for streams with time-based allocations. The connection method is that of peer-to-peer.

1.2 UWB Physical Layer

As mentioned in the previous section, the IEEE 802.15.3 High Rate Alternative PHY Task Group (TG3a) for WPANs is working to define a project to provide a higher speed PHY enhancement amendment to 802.15.3 so as to support very high data rate applications. The goals for this standard are to achieve data rates of up to 110 Mbps at a 10 m distance, 200 Mbps at a 4 m distance, and higher data rates at smaller distances [7]. Based on these requirements, different proposals were submitted in response to 802.15.3a. Most proposals favor the Ultra-Wide-Band (UWB) physical layer. UWB systems have shown their ability to satisfy such needs by providing data rates of up to several hundred Mbps.

UWB was first used to directly modulate an impulse-like waveform with very short duration occupying several gigahertz of bandwidth. Two examples of such systems are

Time-Hopping Pulse Position Modulation (TH-PPM) and Direct-Sequence UWB (DS-UWB). Employing these traditional UWB techniques over the entire allocated frequency band has many disadvantages, including need for high complexity RAKE receivers to capture multipath energy, high-speed analog-to-digital converters (ADC) and high power consumption. These considerations motivated a shift in the UWB system design approach from initial “Single-Band” radio that occupied the entire allocated spectrum in favor of a “Multi-Band” design strategy [2].

“Multi-Band” schemes divide the available UWB spectrum into several sub-bands, each one occupying approximately 500 MHz (which is the minimum bandwidth for a UWB system according to the FCC definition). By interleaving symbols across different sub-bands, a UWB system can still maintain the same transmit power as if it was using the entire bandwidth. A narrower sub-band bandwidth also relaxes the requirement on the sampling rate for ADCs consequently enhancing digital processing capability [2].

Multiband-OFDM (MB-OFDM) is one of the promising candidates for the alternative PHY layer implementation to facilitate WPANs. It combines Orthogonal Frequency Division Multiplexing (OFDM) with the above described multi-band approach enabling UWB transmission so as to inherit all the strengths of an OFDM technique which has already proven its usefulness in wireless communications systems (ADSL, DVB, 802.11a, 802.16.a, etc) [2]. The detailed description of an MB-OFDM UWB system is presented in Chapter 2.

1.3 Multi-Hop Ad Hoc WPAN System

Mobile multi-hop ad hoc networks (MANETs) are collections of mobile nodes connected together over a wireless medium. These nodes can freely and dynamically self-organize into arbitrary and temporary ad hoc network topologies. In this way, devices can seamlessly inter-network in areas where there is no pre-existing communication infrastructure (e.g., disaster recovery sites and battlefield environments). The ad hoc networking concept is not new, having been around for over 30 years in various forms such as packet radio network (1972), survivable adaptive radio network (1980), global mobile information system (early 1990s) [3]. Ad hoc wireless networks, due to their quick and economically less demanding deployment, find applications in several areas. Some of these include military applications, collaborative and distributed computing, emergency operations, wireless mesh networks, wireless sensor networks, and hybrid wireless network architectures [4]. Traditionally, tactical networks have been the only communication networking application that followed the ad hoc paradigm [3].

The principle behind ad hoc networking is that of multi-hop relaying. In a cellular network, the routing decisions are made in a centralized manner with the presence of base stations. But in an ad hoc wireless network, both routing and resource management are done in a distributed manner in which all nodes coordinate to enable communication among the nodes themselves [4]. This requires each node to be more intelligent so that it can function both as a network host for transmitting and receiving data, and as a network router for routing packets from other nodes. Hence, the mobile nodes in ad hoc wireless networks are more complex than their counterparts in cellular networks. The absence of

any central coordinator, or base station, makes the routing process a more complex one compared to that found in cellular networks [4].

Due to the limited transmission range of a wireless network, multiple network “hops” may be needed for one node to exchange data with another node located elsewhere in the network. In such a network, each mobile node operates not only as a host but also as a router, forwarding packets for other mobile nodes in the network that may not be within direct wireless transmission range of each other. Each node participates in a routing protocol that allows it to discover “multi-hop” paths through the network to any other node.

According to the current IEEE 802.15.3 Standard, WPAN is a single-hop network. That is, a data packet can be sent only from a source address to a destination address, and there is no intermediate node to work as a “router”. Using an OFDM UWB physical layer implementation for a WPAN, the range that can be achieved is very limited, usually less than 10 meters. For guaranteed transmission with low packet error rate, a range within 4 meters is usually required. The advantage of a multi-hop network is obvious since it can extend network coverage without increasing either the transmit power, or the receiver sensitivity. The other advantage is that of enhanced reliability via route redundancy.

When the OFDM UWB network topology is changed from a one-hop method to a multi-hop method for coverage, can the QoS requirements still be maintained at an acceptable

level for multimedia traffic? The ability of the IEEE 802.15.3 MAC protocol to facilitate multi-hop networks requires careful and thorough investigation.

An example is used to illustrate why a multi-hop WPAN is needed to provide support for very high-rate real-time traffic flows. A video conference or home theater system is a typical application for use of WPAN based on the OFDM UWB physical layer. That is, the wireless links will be used to transmit the multimedia traffic instead of using cables. The bandwidth requirements for each traffic flow is about 6 Mbps, the average delay should be less than 90 ms, and the packet failure rate should be less than 8% in order to meet the required QoS level. The network area for a video conference or home theater system generally ranges from 9 m x 9 m to 20 m x 20 m. The coverage radius for an OFDM UWB system is approximately only 3 meters for a data rate of 200 Mbps and only 7 meters for a data rate of 480 Mbps to guarantee a PER of 8%. It is obvious that a single-hop network structure is not sufficient to cover the expected network area for these high data rates. If a multi-hop WPAN structure functions well, then the network coverage area can be effectively expanded through the use of intermediate nodes while still maintaining transmission at the needed data rates. The feasibility of the IEEE 802.15.3 TDMA MAC layer for use with multi-hop WPAN systems needs to be validated.

In multi-hop networks, due to the numerous variables involved, the dimensionality of the system grows significantly, thus making analytical modeling a considerably difficult task. Turning to system simulation methods enables the investigation of more complex and realistic phenomena. In a complex system such as multi-hop networks, careful selection

of the system parameters can lead to considerable improvement in performance, especially for time-sensitive applications [6].

Aiming at time-sensitive applications, the goal is to evaluate the performance measures of multi-hop WPAN systems based on an OFDM physical layer. Relevant system performance measures include end-to-end delay, throughput and packet failure rate realized in different situations with different choices of system parameters.

1.4 Challenges Present in Multi-Hop Networks

In a multi-hop ad hoc network, nodes communicate with each other using multi-hop wireless links, and there are no stationary infrastructure components similar to a base station. Each node in the network also acts as a router, forwarding data packets for other nodes. One of the important challenges is the design of dynamic routing protocols that can efficiently find routes between two communication nodes [23]. Routing is obviously the first methodology to be reconsidered in transitioning from single-hop to multi-hop implementations [6]. A mobile ad hoc networking (MANET) working group has been formed within the Internet Engineering Task Force (IETF) to develop a routing framework for IP-based protocols in ad hoc networks [5].

Dozens of routing protocols for MANETs have been proposed, some examples include DSDV (Destination Sequenced Distance Vector), DSR (Dynamic Source Routing), and AODV (Ad-hoc On-demand Distance Vector) [20]. However, most simulations and performance comparisons of mobile ad hoc network routing protocols are based on a simplistic and idealistic physical layer model, as well as simple performance metrics.

Almost all of the existing protocols were designed under the assumption of an UDG (Unit Disk Graph) communication model, in which signal strength fluctuations due to a realistic channel are not considered [17]. Without modification, such routing schemes cannot work well with physical layer characteristics that are representative of more realistic communication channel environments. A detailed discussion of the physical layer impact on the design of the routing protocol can be found in [20] and [24]. The explanation of how the realistic physical layer affects the design of routing protocols will be presented in Chapter 6.

In this study, a position-based stateless routing protocol with greedy forwarding has been implemented for multi-hop WPANs based on a realistic OFDM UWB physical layer. For a WPAN, since it is primarily a home network, most of the nodes will be stationary, and there are no frequent topology updates. Therefore, position-based routing should be a viable approach. Simulation results are obtained to evaluate system performance. These results are used to decide upon the feasibility of employing this routing scheme in multi-hop WPAN scenarios.

Our focus will be on the interaction between the UWB OFDM physical layer and MAC layer. Since the transmission media is a scarce shared resource in a wireless network, controlling access to this shared media efficiently becomes a complicated task. A great deal of effort has been made in this field, and many MAC layer protocols have been proposed. However, few of them were designed to be used in multi-hop wireless links, and very few of them have been evaluated in multi-hop networks.

The IEEE 802.11 MAC protocol is the standard for wireless LANs. In many existing testbeds and network simulation tools for wireless multi-hop ad hoc networks, the protocol for wireless LANs are used. However, this protocol was not designed for multi-hop networks. Although it can support some ad hoc network architectures, it is not intended to support the wireless mobile ad hoc network, in which multi-hop connectivity is one of the most prominent features [5]. Researchers have concluded that the current version of the wireless LAN protocol doesn't function well in multi-hop ad hoc networks. They have presented several serious problems encountered in an IEEE 802.11-based multi-hop network and revealed in-depth causes of these problems in [5]. Hence, it is doubted as to whether the LAN-based system is workable as a mobile ad hoc testbed. Considering typical real-life physical phenomena, and avoiding as many confining assumptions as possible, system performance measures such as delay and packet failure rate have been evaluated for multi-hop ad hoc WLANs in [6]. An important observation in [6] is that, apart from the maximum delay, the results of other performance measurements such as packet failure rate (PFR), indicate that multi-hop WLANs are not promising for real-time applications.

Similar to the IEEE 802.11 WLAN MAC layer, the IEEE 802.15.3 TDMA MAC protocol was not designed for use in multi-hop ad hoc networks. Not much work has been done in multi-hop UWB-based WPAN since the WPAN system is still not mature and the OFDM physical layer proposal has not yet been standardized. A very recent related work [13] describes the design and evaluation of ad hoc extensions to the IEEE 802.15.3 MAC

layer for WPANs. The channel model and physical layer implementation used in the simulations are not described, and a simple radio model in which a node can receive a packet only within the transmission range was used. The motivation in this study is to overcome the situation wherein the past simulation efforts have adopted too many restrictive assumptions, such as an error-free channel, not considering the network layer and transport layer, and a perfect physical layer, etc [6]. A complete and comprehensive simulation environment has been developed in this work spanning both MAC and physical layers that correspond to the IEEE 802.15.3 Standard and the MBOA (MultiBand OFDM Alliance) UWB OFDM proposal. System performance has been evaluated for a variety of different situations as well as for different choices of system parameters.

1.5 Outline of the Dissertation

The remainder of this dissertation is organized as follows. In Chapter 2, the UWB MB-OFDM physical layer is discussed. The UWB radio communication concept is also introduced in this chapter. The MB-OFDM transceiver and related parameters are presented in detail. The BER vs. SNR performance, and the achievable coverage radius of the MBOA OFDM UWB system are discussed at the end of this chapter. Chapter 3 introduces the WPAN MAC layer protocol in detail. The IEEE 802.15.3 Standard MAC is first studied. The channel access scheme of the MAC protocol, TDMA, is then discussed. The complete WPAN system used in our simulations is described in Chapter 4. The simulation modules and protocol stack used in system simulations are given in detail. Performance criteria and QoS requirements are discussed. Network capacity analyses for single-hop and multi-hop WPANs are also presented in this chapter. In

Chapter 5, simulation results for a single-hop WPAN based on the OFDM UWB physical layer are presented. Chapter 6 discusses the design of the routing protocols that are appropriate for a realistic physical layer. A position-based greedy stateless routing protocol for multi-hop WPANs with a realistic OFDM UWB physical layer is adopted in this study. Performance results obtained via computer simulation are given. In Chapter 7, simulation results for various multi-hop WPAN scenarios are presented, and corresponding performance analyses are given. Simulation results and performance analysis for both the equal-weighted node-based scheduling scheme and the on-demand link-based scheduling scheme are presented. Finally, several conclusions are drawn for multi-hop WPANs based on the realistic OFDM physical layer presented in Chapter 8. Some of the relevant future work to be done in related fields is also discussed in Chapter 8.

Chapter 2

OFDM UWB Physical Layer

This chapter describes briefly the Multi-Band OFDM based physical layer proposal of the IEEE 802.15.3a Working Group on short-range high data rate Ultra-Wide-Band (UWB) communications. A brief introduction to UWB radio communications is first given. Then the MB-OFDM PHY layer architecture with the related parameters is described in detail, and optimal choices of critical parameters are discussed. Finally, the physical layer performance of MB-OFDM UWB system is presented, and the coverage radius of UWB OFDM system is also presented for certain specified data rates. The network simulation models were built using Qualnet, a C-language based discrete event network simulator. The implementation of the channel model and physical layer functionalities in Qualnet are discussed in the last section of this chapter.

2.1 Ultra-Wide-Band (UWB) Radio Communications

Bandwidth inadequacy has always been a bottleneck for the development of wireless communication systems as the radio spectrum is a limited resource that is becoming even more valuable. Ultra-Wide-Band (UWB) technology holds great promise for revolutionizing wireless communications. The significant advantages of this technology are low-power operation, mitigated multipath fading effects, high bit-rates and unique precise position/timing location ability [12].

UWB technology is based on the use of very narrow, baseband pulses (typically in order of nanoseconds) as the basic signal structure. These pulses possess spectral components that cover a very wide bandwidth in the frequency domain [12].

Ultra-Wide-Band (UWB) technology was initially used for radars in the 1940s with further significant developments taking place in the 1960s. Recent advances in wireless communications generated a renewed interest in UWB technology (which is alternatively referred as Impulse Radio). Several industries and companies have explored this technology, producing UWB components and devices for wireless communications. The advantages of UWB technology make it attractive for use in a wide set of applications, from Wireless Personal Area Networks (WPANs), Wireless Local Area Networks (WLANs) to ad-hoc networks. Currently, the IEEE 802.15 SG3a (802.15.3a Study Group) is considering the UWB physical layer as a potential candidate for future WPANs [12].

2.1.1 Definition of UWB

The commonly agreed upon definition for UWB transmission is that of a signal whose fractional bandwidth, μ is larger than 0.25, where the fractional bandwidth is defined as

$$\mu = \frac{f_H - f_L}{\left(\frac{f_H + f_L}{2}\right)} \quad (2-1)$$

where f_H and f_L are defined as the highest and lowest frequencies contained in the transmitted signal's spectrum, respectively. The center frequency of the spectrum is

located at $\frac{f_H + f_L}{2}$. Unlike conventional wireless communications systems that are carrier-based, UWB-based communication is baseband using short pulses that spread the energy of the signal from near DC to several GHz.

The low and high frequency limits f_H and f_L need to be defined in less general terms. There may be different ways of selecting these frequencies, depending on how stringent the requirements on the bandwidth are set. In a recent release of UWB emission masks for use in the United States by the Federal Communications Commission (FCC) in 2002, f_L and f_H are set to the lower and upper frequencies of the -10 dB emission points. The selection of -10 dB over the -20 dB bandwidth that was established by the Defense Advanced Research Projects Agency (DARPA) in 1990 is motivated by the fact that UWB emission is permitted at low power levels, which are close to the noise floor. Under these conditions, the -20 dB emission points cannot be measured reliably. According to the regulation of FCC in 2002, a signal is always assumed to be UWB if its bandwidth at the -10 dB emission points exceeds 500 MHz, regardless of the fractional bandwidth value. The 500 MHz bandwidth value is lower than the 1.5 GHz minimum bandwidth limit established by DARPA in 1990. The reduction in bandwidth is due to the use of the -10 dB bandwidth rather than the -20 dB bandwidth that was adopted by DARPA in 1990 [8].

The major differences between UWB technology and existing narrow-band and wide-band technologies are the following:

- The bandwidth of UWB systems, as defined by FCC, is more than 25% of the center frequency, or the bandwidth is greater than 500 MHz.
- The narrow-band and wide-band technologies make use of a radio frequency, whereas the UWB systems are implemented in a carrier-less fashion in which the modulation scheme can directly modulate baseband signals into an impulse with very sharp rise and fall times, thus resulting in a waveform possessing several GHz of bandwidth. These impulses have a very low duty cycle.

With proper emission restrictions in place, the UWB spectrum can overlay onto the existing narrow-band spectrum, resulting in more efficient use of the existing radio spectrum. Figure 2.1 illustrates the upper limits on transmission power permitted for the UWB system in comparison with the IEEE 802.11a Standard [4].

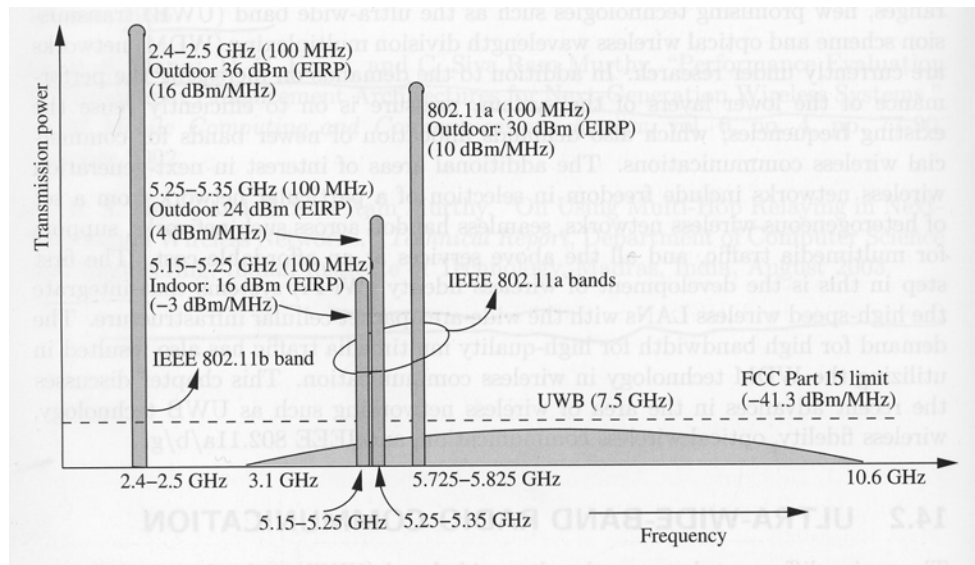


Figure 2.1: Spectrum of UWB Systems Compared With IEEE 802.11b and 802.11a.

2.1.2 UWB Radio Signals

The most common and traditional way of emitting a UWB signal is by radiating pulses that are very short in time. This transmission technique goes under the name of Impulse Radio (IR). The way by which the information data symbols modulate the pulses may vary; Pulse Position Modulation (PPM) and Pulse Amplitude Modulation (PAM) are commonly employed modulation schemes. In addition to modulation, and in order to shape the spectrum of the generated signal, the data symbols are encoded using pseudorandom or pseudonoise (PN) codes. In this common approach, the encoded data symbols introduce a time dither on generated pulses leading to the so-called Time-Hopping UWB (TH-UWB). Direct-Sequence Spread Spectrum (DS-SS), that is, amplitude modulation of basic pulses by encoded data symbols, in the IR version indicated as Direct-Sequence UWB (DS-UWB), also seems particularly attractive. As is well-known, DS-SS has been adopted as the basic radio access technology for third-generation wireless communication systems (UMTS/IMT 2000 in both Europe and Japan) [8].

The UWB definition released by the FCC in 2002, as mentioned in the previous section, does not limit, however, the generation of UWB signals to IR and opens the way, at least in the United States, for alternative non-impulsive schemes. An ultra wide bandwidth, say 500 MHz, might be produced by a very high data rate signal, independently of the characteristics of the pulses themselves. The pulses might, for example, satisfy the Nyquist criterion at an operating pulse rate $1/T$, which would require a minimum bandwidth of $B=1/(2T)$ and thus be limited in frequency, but unlimited in time having the

classical raised-cosine shape with nulls at multiples of $1/T$. Systems with an ultra wide bandwidth of emission due to a high-speed data rate signal rather than a narrow pulse width, provided that the fractional bandwidth or minimum bandwidth requirements are satisfied at all times of the transmission, are not precluded. Methods such as Orthogonal Frequency Division Multiplexing (OFDM) and Multi-Carrier Code Division Multiple Access (MC-CDMA) are capable of generating UWB signals at appropriate data rates [8].

Recent proposals in the United States, and in particular from within the IEEE 802.15.TG3a Working Group, refer to a multi-band (MB) alternative to DS-UWB in which the overall available bandwidth is divided into sub-bands of at least 500 MHz each. The focus of this study is on MB-OFDM. The details of the MB-OFDM physical layer proposal by MBOA (MultiBand OFDM Alliance) are described in the next section.

2.2 MBOA Multi-Band OFDM Physical Layer Proposal

Multi-band OFDM is a transmission technique wherein the available spectrum is divided into multiple bands. Information is transmitted on each band using OFDM modulation. The available spectrum (3.1-10.6 GHz) is divided into 13 bands of 528 MHz each. Channelization in MB-OFDM is achieved by using different time-frequency codes, each of which is a repetition of an ordered group of channel indices [14].

The UWB system provides a wireless personal area communications network with data payload capabilities of 53.3, 80, 110, 160, 200, 320, 400, and 480 Mbps. Support for transmitting and receiving at data rates of 53.3, 110 and 200 Mbps is mandatory. The

proposed UWB system employs OFDM using a total of 122 modulated and pilot subcarriers out of a total of 128 subcarriers. Forward error correction coding by means of convolutional coding is used with coding rates of $1/3$, $11/32$, $1/2$, $5/8$, and $3/4$.

The proposed UWB system also utilizes a time-frequency code (TFC) to interleave coded data over a maximum of three frequency bands (called a Band Group). Four such Band Groups with three bands each as well as one Band Group with two bands are defined, along with four 3-band TFCs and two 2-band TFCs. Together, these Band Groups and the TFCs provide the capability to define eighteen separate logical channels or independent piconets. Devices operating in Band Group #1 (the three lowest frequency bands) are denoted Mode 1 devices. It is mandatory for all devices to support Mode 1 operation. Support for the other Band Groups is optional and can be added in the future [11].

The data rate-dependent modulation parameters for the MBOA OFDM UWB physical layer are listed in Table 2.1.

Data Rate (Mb/s)	Modulation	Coding Rate (R)	Time Spreading Factor (TSF)	Overall Spreading Gain	Coded bits per OFDM Symbol (N_{CBPS})
53.3	QPSK	1/3	2	4	100
80	QPSK	1/2	2	4	100
110	QPSK	11/32	2	2	200
160	QPSK	1/2	2	2	200
200	QPSK	5/8	2	2	200
320	QPSK	1/2	1 (No spreading)	1	200
400	QPSK	5/8	1 (No spreading)	1	200
480	QPSK	3/4	1 (No spreading)	1	200

Table 2.1: Rate-Dependent Parameters for the MBOA OFDM UWB Physical Layer.

2.2.1 Mathematical Description of the OFDM Signal

The transmitted RF signal is related to the baseband signal as follows

$$r_{RF}(t) = \text{Re} \left\{ \sum_{k=0}^{N-1} r_k(t - kT_{SYM}) \exp(j2\pi f_{(k \bmod 6)} t) \right\} \quad (2-2)$$

where, $\text{Re}(\cdot)$ represents the real part of a complex number, $r_k(t)$ is the (possibly complex) baseband signal representing the k^{th} OFDM symbol occupying a symbol interval of length T_{SYM} , and N is the number of OFDM symbols transmitted. The carrier frequency or band on which the k^{th} OFDM symbol is transmitted is denoted as f_k . The values of f_k range over the three frequencies assigned to the Band Group within which the system is

operating. These frequencies are organized into sequences of length six, which are called time-frequency codes (TFCs).

All of the OFDM symbols $r_k(t)$ can be constructed using an inverse Fourier transform with a certain set of coefficients C_n , where the coefficients are defined as either data, pilots, or training symbols. The OFDM symbols are given according to

$$r_k(t) = \begin{cases} \sum_{n=-N_{ST}/2}^{N_{ST}/2} C_n \exp(j2\pi n \Delta_f t) & t \in [0, T_{FFT}] \\ 0 & t \in [T_{FFT}, T_{FFT} + T_{ZP}] \end{cases} \quad (2-3)$$

where the parameters Δ_f and N_{ST} are defined as the subcarrier frequency spacing and the number of total subcarriers used, respectively. The resulting waveform has a duration of $T_{FFT} = 1/\Delta_f$ seconds. The time parameter T_{ZP} specifies a zero pad period for the OFDM symbol that is used to mitigate the effects of multipath fading as well as to provide a guard period to allow for switching between the different bands [11].

2.2.2 OFDM Modulation and Parameters

For the OFDM modulation used here, the FFT size is set to 128. There are 100 data carriers out of 122 total sub-carriers in each OFDM symbol. A total of 12 sub-carriers are pilot carriers, which are dedicated to pilot signals that are used to mitigate the effects of frequency offsets and phase noise. There are 10 sub-carriers at the edges of the occupied frequency band to serve as guard carriers.

A guard interval is added to the cyclic prefix to switch between sub-bands. The cyclic prefix is a zero padded (ZP) interval that is appended at the end of the OFDM symbol, so as to reduce the effects of Inter-Symbol Interference (ISI) between OFDM symbols. The guard interval (GI) is added after the zero padded interval [10].

The OFDM subcarriers are modulated using QPSK. The encoded and interleaved binary serial input data are divided into groups of two bits and converted into complex numbers representing QPSK constellation points. The conversion is performed using a Gray-coded constellation mapping strategy. The output values, d , are formed by multiplying the resulting $(I + jQ)$ value by a normalization factor of K_{MOD} , as described in the following equation

$$d = (I + jQ) \times K_{MOD}. \quad (2-4)$$

The normalized factor, K_{MOD} , depends on the modulation mode. For QPSK modulation, the value of K_{MOD} is taken to be $1/\sqrt{2}$.

For information data rates of 53.3 and 80 Mb/s, the stream of complex-valued symbols is divided into groups of 50 complex numbers. We shall denote these complex numbers $c_{n,k}$, which corresponds to subcarrier n of OFDM symbol k , as follows

$$\begin{aligned} c_{n,k} &= d_{n+50 \times k} & n &= 0, 1, \dots, 49 \\ c_{(n+50),k} &= d_{(49-n)+50 \times k} & k &= 0, 1, \dots, N_{SYM} - 1 \end{aligned} \quad (2-5)$$

where N_{SYM} denotes the number of OFDM symbols in the MAC frame body, tail bits, and pad bits.

For information data rates of 110, 160, 200, 320, 400 and 480 Mbps, the stream of complex numbers is divided into groups of 100 complex numbers. The complex number $C_{n,k}$ corresponds to subcarrier n of OFDM symbol k , and is denoted as follows

$$C_{n,k} = d_{n+100 \times k} \quad \begin{array}{l} n = 0, 1, \dots, 99 \\ k = 0, 1, \dots, N_{SYM} - 1 \end{array} \quad (2-6)$$

where N_{SYM} denotes the number of OFDM symbols in the MAC frame body tail bits, and pad bits.

The timing parameters associated with the OFDM physical layer are listed in Table 2.2.

Parameter	Value
N_{SD} : Number of data subcarriers	100
N_{SDP} : Number of defined pilot carriers	12
N_{SG} : Number of guard carriers	10
N_{ST} : Number of total subcarriers used	122 (= $N_{SD} + N_{SDP} + N_{SG}$)
Δ_F : Subcarrier frequency spacing	4.125 MHz (= 528 MHz/128)
T_{FFT} : IFFT/FFT period	242.42 ns (= $1/\Delta_F$)
T_{ZP} : Zero pad duration	70.08 ns (= $37/528$ MHz)
T_{SYM} : Symbol interval	312.5 ns (= $T_{CP} + T_{FFT} + T_{GI}$)

Table 2.2: Timing-Related Parameters for the MBOA OFDM UWB Physical Layer.

2.2.3 Transmission Modes and Access Schemes

The proposed UWB system utilize five sub-band groups formed with 3 frequency bands (called a Band Group) and time-frequency codes (TFC) to interleave and spread coded data over 3 frequency bands. Four such Band Groups with 3 bands each and one Band Group with 2 bands are defined within the UWB spectrum mask [10]. Band Group 1 is used for Mode 1 devices (mandatory mode). The remaining Band Groups are reserved for future use. The frequency band allocation is summarized in Table 2.3, and the frequency of operation for Mode 1 devices is shown in Figure 2.2.

Band Group	BAND_ID	Lower frequency	Center frequency	Upper frequency
1	1	3168 MHz	3432 MHz	3696 MHz
	2	3696 MHz	3960 MHz	4224 MHz
	3	4224 MHz	4488 MHz	4752 MHz
2	4	4752 MHz	5016 MHz	5280 MHz
	5	5280 MHz	5544 MHz	5808 MHz
	6	5808 MHz	6072 MHz	6336 MHz
3	7	6336 MHz	6600 MHz	6864 MHz
	8	6864 MHz	7128 MHz	7392 MHz
	9	7392 MHz	7656 MHz	7920 MHz
4	10	7920 MHz	8184 MHz	8448 MHz
	11	8448 MHz	8712 MHz	8976 MHz
	12	8976 MHz	9240 MHz	9504 MHz
5	13	9504 MHz	9768 MHz	10032 MHz
	14	10032 MHz	10296 MHz	10560 MHz

Table 2.3: Band Allocation for the MBOA OFDM UWB Physical Layer.

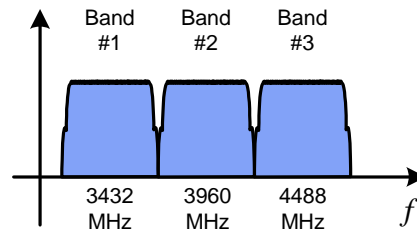


Figure 2.2: Frequency of Operation for a Mode 1 Device.

2.2.4 Receiver Sensitivity

For a value of packet error rate (PER) less than 8% for a packet size of 1024 bytes, the minimum receiver sensitivity values in dBm for the various data rates and modes are listed in Table 2.4.

Data Rate (Mb/s)	Minimum Sensitivity (dBm) for Mode 1
53.3	-83.6
80	-81.6
110	-80.5
160	-78.6
200	-77.2
320	-75.5
400	-74.2
480	-72.6

Table 2.4: Receiver Performance Requirements for the MBOA OFDM UWB Physical Layer.

2.3 Performance of the MBOA OFDM UWB Physical Layer

The MBOA air interface is based on the classical configuration for coded OFDM system.

The multi-band processing is achieved by switching OFDM symbols from one sub-band

to another. The operating Band Group and sub-bands are identified by Time Frequency Codes that specify the frequency hopping pattern associated with each piconet. The MBOA OFDM transmitter is shown in Figure 2.3.

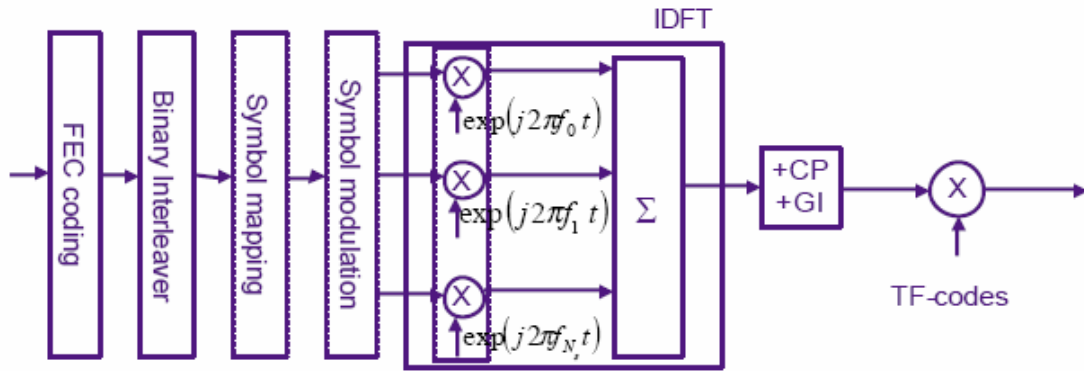


Figure 2.3: MBOA OFDM Transmitter [10].

Using the common channel models (CM1-CM4) proposed in [7], much work has been done to evaluate the performance of the MB-OFDM UWB system. In [10], a bit error rate (BER) performance analysis of the UWB-OFDM proposal is provided. The results reported are considered to be the most complete that are available to date. The BER results are given following the MB-OFDM specifications proposed for the four propagation scenarios, CM1 to CM4. The cutoff threshold applied on the impulse response of the channel is either set to 10 dB, or 20 dB below the highest peak of the Average Power Delay Profile of the channel. From performance curves found in [10], it can be observed that the BER performance for the four channel environments CM1-CM4 are very similar for a specified data rate. For the -10 dB threshold power level, the BER curves are shown in Figure 2.4 for several transmission modes over the CM1 channel.

The BER is plotted as a function of the ratio of the useful energy per bit to the noise level, i.e., E_b/N_0 .

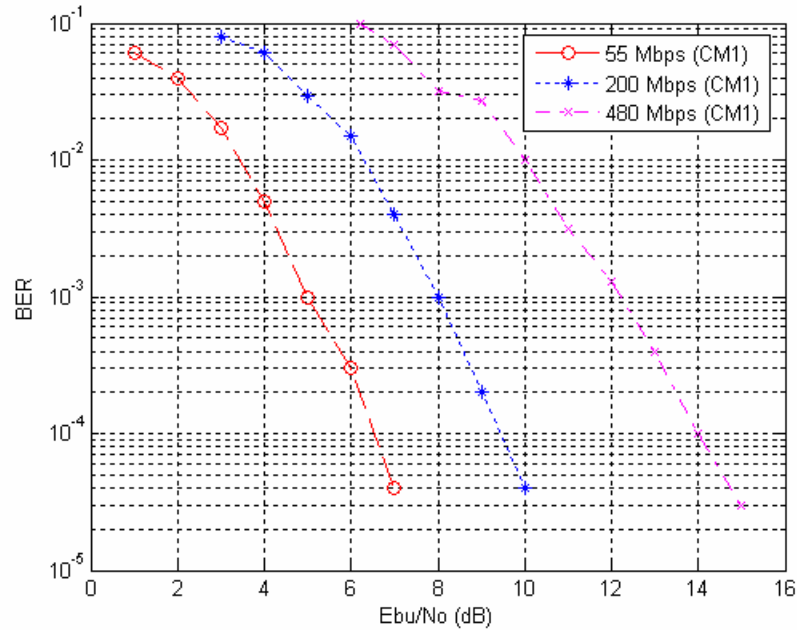


Figure 2.4: BER Performance vs. E_b/N_0 for CM1 Channel.

2.4 Coverage Radius of the MBOA OFDM System

The physical layer performance measured in terms of packet error rate with respect to coverage radius of the Multi-Band OFDM system was presented by the Multi-Band OFDM Alliance (MBOA) for both AWGN and multipath channel environments in the 802.15.3a channel modeling sub-committee report. The range at which the Multi-Band OFDM system, operating in Mode 1, can achieve a PER of 8% with a link success probability of 90% is listed in Table 2.5 for the AWGN and the multipath channel environments. The data in Table 2.5 were obtained from [11].

Rate	AWGN	CM1	CM2	CM3	CM4
110 Mb/s	21.4 m	12.0 m	11.4 m	12.3 m	11.3 m
200 Mb/s	14.6 m	7.4 m	7.4 m	7.5 m	6.6 m
480 Mb/s	9.3 m	3.2 m	3.2 m	N/A	N/A

Table 2.5: Range to Achieve a PER of 8% With a 90% Link Success Probability for Mode 1 Devices [11].

In the AWGN channel and all multipath channel environments, the MBOA OFDM system can support data rates of 110 Mbps at a distance of 10 m and 200 Mbps at a distance of 4 m. Furthermore, this MBOA OFDM system can support data rates of 110 Mbps, 200 Mbps and 480 Mbps at a distance of 11.3-12.3 m, 6.6-7.5 m and 3.0 m, respectively, in the various multipath channel environments (CM1–CM4) while achieving a link success probability of 90%. Systems operating at a data rate of 53.3 Mbps and 110 Mbps exhibit similar performance. The range at which the PER is 8% for 53.5 Mbps transmission systems in multipath environments is around 12 m [11].

2.5 Physical Layer Implementation Using Qualnet

The network simulation models were implemented using Qualnet in this study. Qualnet is a C language-based, discrete-event network simulator. An introduction to Qualnet is presented in Section 4.1. Qualnet provides two packet reception models within the physical layer: BER-based and SNR-Threshold-based. For the BER-based model, the receiver looks up bit error rate (BER) values in the SNR-BER table to calculate the packet error rate (PER). For the SNR-Threshold based model, if the Signal-to-Noise Ratio (SNR) at the receiver is more than the specified threshold, the receiver demodulates

and processes the signal without error. Otherwise, the packet is dropped. The BER-based model is used in this study.

A realistic UWB channel is simulated in this study by using free space, shadowing, and Rayleigh fading channel model components at the same time. The corresponding channel BERs are extracted from the BER vs. SNR curves for a 10 dB threshold cutoff level in the case of CM1 as shown in Figure 2.4. From the BER values given in [10], it can be observed that the BER performances for the four channel environments CM1-CM4 are very similar for the specified data rate. Therefore, using the BER-SNR curve for CM1 at the specified data rate will not appreciably affect the network performance.

Chapter 3

WPAN MAC Layer

This chapter outlines the design of the Medium Access Control (MAC) layer that is compatible with the IEEE 802.15.3 Standard. The major issues to be considered in designing a MAC protocol for a wireless ad hoc network are introduced first. Then the IEEE 802.15.3 MAC layer protocol is presented in detail. The basic concepts related to, and scheduling schemes for, the TDMA (Time Division Multiple Access) MAC protocol are also discussed. Finally, we describe the implementation of the MAC layer protocol using the Qualnet software simulation tool.

3.1 MAC Layer Protocol

Nodes in an ad hoc wireless network share a common broadcast radio channel. Since the radio spectrum is limited, the bandwidth available for communication in such a network is also limited. Access to this shared medium should be controlled in such a manner that all nodes receive a fair share of the available bandwidth, and that the bandwidth is utilized efficiently [4]. Therefore, the primary responsibility of the MAC protocol in a wireless network is that of channel access for the transmission of data packets. The performance of any wireless network hinges on the MAC protocol, more so for ad hoc wireless networks. The major issues to be considered in designing a MAC protocol are as follows:

- **Synchronization:** The MAC protocol design should take into account the requirement of time synchronization. Synchronization is mandatory for TDMA-

based systems in order to enable the management of transmission and reception time slots.

- **Throughput:** The MAC protocol employed in ad hoc wireless networks should attempt to maximize the throughput of the system. The important considerations for throughput enhancement are minimizing the occurrence of collisions, maximizing channel utilization, and minimizing control overhead.
- **Access Delay:** The access delay refers to the average delay that any packet encounters awaiting transmission. The MAC protocol should attempt to minimize the access delay.
- **Fairness:** Fairness refers to the ability of the MAC protocol to provide an equal, or weighted, share of the bandwidth to all competing nodes. Fairness can be either node-based, or flow-based. The former attempts to provide an equal bandwidth share for competing nodes, whereas the latter provides an equal share for competing data transfer sessions.

3.2 IEEE 802.15.3 MAC Layer

All data in the IEEE 802.15.3 piconet are exchanged in a peer-to-peer manner. That is, data are communicated directly between source node and destination node after a PNC (piconet controller) broadcasts a beacon that includes the time allocation of the superframe. Timing in the IEEE 802.15.3 piconet is based on the superframe, which is illustrated in Figure 3.1.

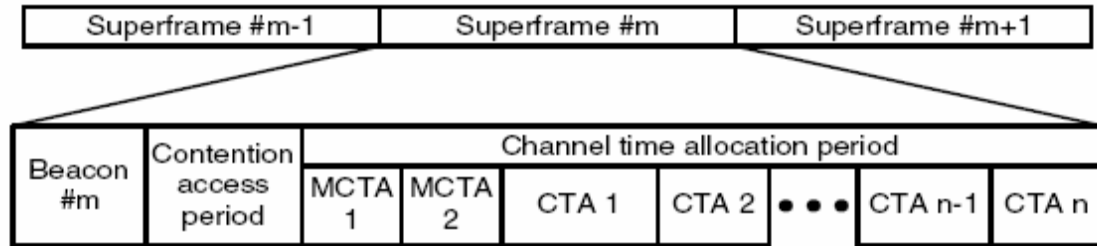


Figure 3.1: Superframe Structure in an IEEE 802.15.3 Piconet.

The channel time is divided into superframes, wherein each superframe begins with a beacon. The superframe is composed of three major parts: the beacon, the optional CAP and the CTAP, as shown in Figure 3.1. A brief description of each part is as follows:

- The beacon is used to set the timing allocations and to communicate management information throughout the piconet. The beacon consists of the beacon frame, as well as any Announce commands sent by the PNC as a beacon extension.
- The optional Contention Access Period (CAP) is used to communicate commands and/or asynchronous data if they are present in the superframe.
- The channel time allocation period (CTAP), which is also called the contention free period, is composed of channel time allocations (CTAs), including management CTAs (MCTAs). The CTAs are used for commands, isochronous streams and asynchronous data connections.

In Figure 3.1, the MCTAs are shown first, but the PNC is allowed to place any number of them at any position within the superframe.

The length of the CAP is determined by the PNC and communicated to the nodes within the piconet via the beacon. However, the PNC is able to replace the functionality provided in the CAP with management CTAs (MCTAs). MCTA is a type of CTA that is used for communications between the nodes and the PNC.

The CAP uses Carrier Sense Multiple Access with Collision Avoidance (CSMA/CA) for the medium access. The CTAP, on the other hand, uses a standard TDMA protocol where the nodes have specified time windows. MCTAs are either assigned to a specific source/destination pair and use TDMA for access, or they are shared CTAs that are accessed using the slotted ALOHA protocol.

Since CAP is an optional section during each superframe, we only consider the access scheme based on TDMA in this study. The CTA time slots are allocated by the PNC. Each CTA is defined by a start time and a duration value so that each node knows when and how long it can transmit. During the contention free period of the IEEE 802.15.3 MAC protocol, the guard times are used to keep transmissions in adjacent CTAs from colliding.

Three ACK policies are defined in the IEEE 802.15.3 Standard: Imm-ACK, No-ACK, and Dly-ACK. For the Imm-ACK policy, the receiver issues an ACK frame to the

transmitter for every received packet. No-ACK means no ACK frame is issued; while Dly-ACK is the tradeoff between the No-ACK and Imm-ACK. The receiver issues an ACK frame for multiple received packets. In our simulations, the No-Ack policy has been implemented for the sake of simplicity.

3.3 Basics of Time Division Multiple Access (TDMA)

Time Division Multiple Access (TDMA) shares the available bandwidth in the time domain. Each frequency band is divided into several time slots (channels). A set of such periodically repeating time slots is known as the TDMA frame. Each node is assigned one or more time slots in each frame, and the node transmits only in those time slots [4].

For two-way communication, the uplink and downlink time slots, used for transmitting and receiving data, respectively, can be on the same frequency band (TDMA frame) or on different frequency bands. Though TDMA is essentially a half-duplex mechanism, where only one of the two communicating nodes can transmit at a time, the small time duration of the time slots creates the illusion of a two-way simultaneous communication. Perfect synchronization is required between the sender and the receiver. To prevent synchronization errors and inter-symbol interference due to signal propagation time differences, guard intervals are introduced between time slots. Since the sizes of slots are already small, the introduction of guard intervals results in a significant increase in overhead for the overall system.

For the IEEE 802.15.3 WPAN system, the information is maintained by a distributed beaconing procedure in which each device has a chance of sending a beacon at the

beginning of a superframe but only one device in a local region actually does. A device synchronizes its clock with the information contained in a detected beacon [13]. In our simulations, the global synchronization scheme is employed between ad-hoc devices for convenience.

3.4 Scheduling in TDMA

In IEEE 802.15.3, the assignment of time slots (CTAs) to nodes is done by a PNC. The algorithm used to allocate the channel time and assign CTAs is outside of the scope of the published Standard. Choice of an appropriate TDMA scheduling algorithm is left to the system designers to devise and implement.

The overall problem of finding good scheduling schemes plays an important role in TDMA system design, and it affects many network performance metrics such as bandwidth efficiency, throughput, delay, and fairness.

The main task in designing a TDMA schedule is to allocate time slots depending on the topology and the node packet generation rates. A proper scheduling algorithm not only avoids collisions by silencing the interferers of every receiver node in each time slot but also by minimizing the number of time slots, and hence, the overall system latency [14].

To allocate each source node with fixed time slots is the most straightforward method. The node-based equal-weighted algorithm is used first in our simulations. Each node is assigned a time slot. The number of time slots within a TDMA time frame is taken to be the total number of nodes in this study. The advantages and disadvantages are obvious for

this method. The source node will still be allocated time slots even if it has no data to send. Thus, the bandwidth is wasted unnecessarily. When there are only a few independent point-to-point flows in the network, the channel bandwidth efficiency is very low. On the other hand, this method can transmit data in a timely manner when needed because a source node will have time slots available to send data that may suddenly arrive without the need to request any time slots in advance.

Another way to allocate the time slots is based on the traffic flow (or link). An on-demand scheduling scheme is one such kind of link-based scheduling algorithm. When a node has packets to send, a greedy search for the unused time slots will be performed. If there are unused time slots found to be available during a frame, one time slot will be selected randomly and assigned to the requesting node. When all the time slots are used up, the requesting node cannot have any time slots assigned, and the packets will then be dropped [17]. The slot number per frame is fixed during one simulation iteration. However, the slot number per frame is different for different multi-hop scenarios.

3.5 Implementation of the TDMA MAC Layer Using Qualnet

In the simulations conducted in this study, only the TDMA channel access method is considered, and only data frames are transmitted and received. No acknowledgement is implemented. Global synchronization throughout the network is implemented by using a global timer in the Qualnet network simulation tool.

Chapter 4

WPAN System Description

In this chapter, we present the details of the overall WPAN system that is used in the simulations. First, the general system description for the WPAN system is given. Then the QoS requirements are presented and the performance criteria are discussed. Finally, the network capacity analyses for both single-hop and multi-hop WPANs are presented in detail.

4.1 Description of the Overall System

The network simulation models were implemented using Qualnet. Qualnet is a commercial product available from Scalable Network Technologies (SNT), which is derived from GloMoSim. GloMoSim is a scalable simulation library that was designed at the University of California Los Angeles Computing Laboratory to support studies of large-scale network models. SNT then expanded and further developed GloMoSim to produce the Qualnet product. Although Qualnet is based on GloMoSim, it dramatically expands its capabilities in terms of model libraries and protocols, graphical tools for experiment planning, analysis and visualization, as well as, in terms of available documentation and technical support.

Qualnet is a network modeling software package that predicts performance of networks through simulation and emulation. It is a C language-based discrete-event simulator. Qualnet uses a layered architecture similar to that of the TCP/IP network protocol stack. Within that architecture, data moves between adjacent layers. Each node in Qualnet runs

a protocol stack. Each layer provides a service to the layer above it, by using the services of the layers below it. Each protocol operates at one of the layers of the stack. Protocols in Qualnet essentially operate as a finite state machine. The occurrence of an event corresponds to a transition from one state to another within the finite state machine [27].

In the simulations, the following assumptions have been made:

- All nodes are homogenous and stationary.
- Each node can have multiple connections to the same destination.

A number of n nodes with limited buffer size are uniform-randomly located inside a rectangular area, laid diagonally between (x_{min}, y_{min}) and (x_{max}, y_{max}) . The upper and lower limits, together with the transmitter's wireless range, determine whether either a single hop, or a multi-hop scenario is to be employed for communication between the source-destination pair.

In the simulations performed in this study, n is fixed at the value of 20. For home networking, a total of 20 nodes is quite sufficient to reflect a realistic wireless personal area network. Randomly selected nodes are responsible for generating traffic, while all nodes might serve as forwarding and final destination nodes at any time during the simulation. Each active node has a pre-assigned final destination node that remains unchanged throughout the course of the simulation. This is not considered to be either a simplifying, or restrictive assumption since all the nodes are randomly located and uniformly distributed over the area covered by the communication network [6].

All nodes broadcast their transmissions omni-directionally. Antenna effects are not considered in this study. Hence, the antenna efficiency is set to unity, and the losses caused by an antenna are set to 0 dB.

The packet generation rate at the application layer of each node is modeled as a Poisson process. The mean packet generation rate for each active link ranges from 128 kbps to 6 Mbps. This range reflects the throughput requirements for a typical real-time Variable Bit Rate (VBR) application. The number of source-destination pairs, together with the packet generation rate per link, serves as the system's traffic volume indicator. For a multi-hop network, the data are transmitted from the source node to the destination node through several wireless links. One source-destination pair refers to one traffic flow traversing from the source to the destination, no matter which path is used and how many links are utilized. The number of source-destination pairs refers to the number of traffic flows. In some literature, the number of source-destination pairs is synonymous with the term active link numbers. In our simulations, a total of 2 to 10 active links are implemented.

The size of a TDMA time slot is equal to the transmission duration of one packet for a specified data rate. The slot number per frame is not fixed and can change depending on the specific network scenario. For single-hop scenarios, only the nodes that have packets to send are assigned time slots. Hence, the slot number per frame is taken to be the link number, and the scheduling efficiency will be close to 100%. For multi-hop scenarios, the slot number per frame depends on the scheduling scheme that is being employed. For equal-weighted node-based scheduling, the slot number per frame is taken to be the total

number of nodes in the network. For on-demand link-based scheduling, the slot number per frame is fixed during one simulation. However, the slot number per frame is different for different multi-hop scenarios.

The network layer protocol used in our system simulation is IP version 4. The transport layer protocol used currently is the User Datagram Protocol (UDP). The UDP protocol provides a way for applications to send IP datagrams and send them without having to establish a connection.

A realistic UWB channel is simulated in our study by using free space, shadowing, and Rayleigh fading channel model components concurrently. Only frequency Band #1 within Band Group 1 is considered in this study. The corresponding specifications for this frequency band were described in Section 2.4. Hence, with a center frequency of 3.432 GHz and a bandwidth of 528 MHz, the lower frequency is 3.168 GHz, and the upper frequency is 3.696 GHz. The channel bit error rates are extracted from the BER vs. SNR curve for the CM1 channel environment as described in Section 2.6. The BER curves used in the simulations were shown in Figure 2.3 of Section 2.4.

The protocols for the different network layers are as follows:

- Application Layer: VBR (Variable Bit Rate).
- Transport Layer: UDP.
- Network Layer: IP version 4.
- MAC Layer: IEEE 802.15.3 TDMA Protocol.

- Physical Layer: MBOA UWB OFDM physical layer for IEEE 802.15.3a.

4.2 Quality-of-Service Requirements

The main purpose of the UWB 802.15.3 network is to transmit multimedia traffic. For multimedia applications, it is important that certain Quality-of-Service (QoS) targets be met. Table 4.1, taken from [15], shows typical QoS requirements for several service classes: non-real-time variable bit rate (nrt-VBR), available bit rate (ABR), unspecified bit rate (UBR), constant bit rate (CBR) and real-time VBR (rt-VBR). Some example applications are also listed in Table 4.1.

Class	Application	Bandwidth (b/s)	Delay Bound (ms)	Bit Loss Rate
CBR	Voice	32k – 2M	30 - 60	10^{-2}
nrt-VBR	Digital video	1M – 10M	Large	10^{-6}
rt-VBR	Video	128k – 6M	40 - 90	10^{-3}
UBR	File transfer	1M – 10 M	Large	10^{-8}
ABR	Web browsing	1M – 10M	Large	10^{-8}

Table 4.1: QoS Requirements for Different Applications.

4.3 System Performance Criteria

End-to-end average delay and packet failure rate (PFR) are two major performance indicators that are used in this study.

The delay includes the time duration from the moment that a packet is generated until it is correctly received. In each simulation run, delay is calculated by averaging over all

correctly received packets. In our simulations, the delay consists of the transmission delay, propagation delay, and the queueing delay. The packetization delay and all other processing delays are not considered, since they are both fixed and negligible compared to the random transmission and queueing delays.

In a wireless communications system, propagation delay refers to the time taken for a signal to travel from its source to its destination. Propagation delay is dependent solely on the distance the signal has to travel and on the signal's speed. That is,

$$\text{Propagation delay} = \frac{L}{V} \quad (4-1)$$

where L is the length of the link, and V is the propagation speed of signal over the link. The propagation speed depends on the physical medium of the link, and is in the range from 2×10^8 m/s to 3×10^8 m/s. Hence, the propagation delay is generally on the order of nanoseconds. Generally, it is fixed and negligible compared with the transmission delay and queueing delay.

Transmission delay is the time that is required to transmit a block or a frame of data at a specified data rate. That is,

$$\text{Transmission delay} = \frac{S}{R} \quad (4-2)$$

where S is the size of the data being transmitted in bits, and R is the transmission rate in bits/second. Generally, the transmission delay is related to both the packet length and the transmission rate.

Queueing delay is the delay from the point of entry of a packet in the transmission queue to the actual point of transmission. This delay depends upon the load that is present on the communication link and the size of queue. Generally, the queueing delay is proportional to the network buffer size. The longer the line of packets waiting to be transmitted, the longer will be the average waiting time. However, this situation is preferred compared to the use of a short buffer, which would result in dropped packets.

Packet failure rate (PFR) is the ratio of the number of packets dropped normalized by the total number of generated packets throughout the duration of a simulation. Different limit violations, such as the network buffer size, time to live (TTL) value in the IP protocol, and the hop limit in routing protocols, in the aggregate contribute to the total number of dropped packets. Generally, packet losses are due to the following reasons: channel error, buffer overflow and collisions.

Channel errors are caused by signal distortions that occur during propagation over the radio channel. Such distortions include path loss, slow and fast fading, etc. Packet error rate (PER) is the quantitative indicator of the channel error condition that is present in a wireless communications system. If the packet error rate is over a certain threshold value

at the receiver side, the packet will be dropped. Therefore, an increasing number of channel errors results in more dropped packets. That is, a higher PER will lead to a higher PFR. Network buffers are used for flow control in wireless communications systems. A buffer overflow occurs when the network layer attempts to store more packets in a fixed length transmission buffer than it was intended to hold. The packets will be dropped when the buffer is full. If two or more nodes send a packet in a given time slot, then there is a collision and the receiver obtains no information about the transmitted packets. Since TDMA is collision-free theoretically, the scheduling scheme guarantees that only one node can transmit within any one time slot. Also, both a guard time and an intra-frame time are implemented in the TDMA MAC layer so as to prevent the transmissions from colliding. Hence, the number of packet failures due to a collision is negligible here compared with packet failures caused by channel error events and buffer overflow conditions.

4.4 Network Capacity of a Single-Hop WPAN

In this section, a simple single-hop network scenario has been simulated to test whether the saturation throughput, which is the achievable throughput when the network saturation is reached, will match those presented in the MBOA OFDM proposal [11] for peer-to-peer communications. In this simple scenario, transmission systems operating at 53.3 Mbps and 200 Mbps have been tested. A total of only two source-destination pairs are present within the network active area to obtain the saturation throughput. The network range is bounded by a $4\text{m} \times 4\text{m}$ square area, which means that the two randomly distributed nodes are very close. Here, the two nodes are so close that the transmission error could be negligible, and the packet failures are caused only by buffer overflow after

saturation of the network has been reached. This is not typical in most wireless communications environments. The purpose of this configuration is to test the saturation throughput, and hence, only the system throughput is measured in this situation.

The number of slots per frame is set to the value of 2, which is the number of source-destination pairs. Each active source node is assigned a time slot within one frame. In this simple scenario, the scheduling efficiency is very close to 100%. When the transmission error can be neglected, the saturation throughput in this scenario should be a reasonable approximation to the achievable total throughput of the system at the application layer.

The packet size at the application layer is 1024 bytes. When the packet generation rate increases from 0.1 to 100,000 packets/s per link, the throughput will increase accordingly and eventually reach saturation at a certain point. Once the saturation throughput is reached, the overflowed packets will be discarded from the network queue. Simulation results for the total throughput versus packet rate per link are shown in Figure 4.1.

It can be observed that the saturation throughput for the transmission scheme operating at 53.3 Mbps is actually 44.1 Mbps. Also, the saturation throughput for the transmission scheme operating at 200 Mbps is actually 121.7 Mbps.

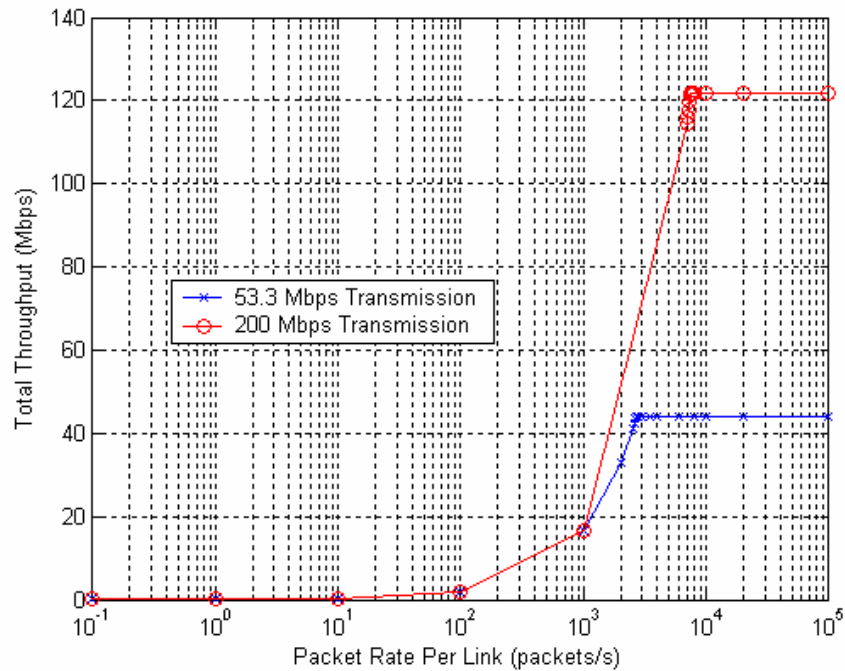


Figure 4.1: Total Throughput vs. Packet Generation Rate Per Link.

The achievable PHY layer throughputs for a 1024-byte packet for the OFDM UWB physical layer proposed by the MBOA were presented in [11]. The data in Table 4.2 were obtained from [11] and summarize the key results.

Number of Frames	Throughput at 53.3 Mbps	Throughput at 200 Mbps	Throughput at 480 Mbps
1	45.8 Mb/s	127.3 Mb/s	195.6 Mb/s
5	48.4 Mb/s	149.3 Mb/s	253.0 Mb/s

Table 4.2: Throughput for a 1024 Byte Packet vs. Data Rate (single/multiple frames).

The application layer throughput is expected to be slightly lower than the throughput for the physical layer, because of the presence of header bits in other layers (IP, MAC etc),

along with the Guard time and Inter-frame time used in the MAC layer. Therefore, it can be said that the application layer throughput performance presented in Figure 4.1 is reasonable, and the throughput performance of the UWB physical layer and TDMA MAC layer developed in this study match those presented in the MBOA OFDM proposal.

4.5 Capacity Analysis of a Multi-Hop Network

The network throughput or aggregate capacity for a multi-hop network is discussed in this section. When frequency reuse is not considered, the capacity of multi-hop networks is greatly affected by the average hop count h . Theoretically, if the network capacity based on peer-to-peer communications is C , the capacity of multi-hop networks will be roughly $C_{multi} = C/h$, assuming that the network bandwidth used for routing messages is negligible, and that a high-efficiency scheduling scheme is implemented. If the average packet generation rate is r Mbps, the maximum number of source-destination pairs that can be supported is $L_{max} = \lfloor C_{multi}/r \rfloor$. When the number of source-destination pairs L is over L_{max} , packets will be dropped due to the presence of a network saturation condition [17].

The transmission system operating at 200 Mbps is used here to illustrate how the multi-hop network capacity is related to the peer-to-peer network capacity and the average hop count. As known from Section 4.4, the achievable throughput for 200 Mbps peer-to-peer transmission is about 120 Mbps. If the average hop count is set to $h = 3$, the capacity of a multi-hop network will be $C_{multi} = 120/3 = 40$ Mbps, theoretically. If the average packet generation rate per link is $r = 6$ Mbps, then the maximum number of source-destination pairs that can be supported is $L_{max} = \lfloor C_{multi}/r \rfloor = \lfloor 40/6 \rfloor = 6$. If the packet generation rate

per link is $r = 3$ Mbps, then the maximum number of source-destination pairs that can be supported is $L_{max} = \lfloor C_{multi}/r \rfloor = \lfloor 40/3 \rfloor = 13$. If the average hop count is set to $h = 4$, the capacity of a multi-hop network will be $C_{multi} = 120/4 = 30$ Mbps, theoretically. If the average packet generation rate per link is $r = 6$ Mbps, then the maximum number of source-destination pairs that can be supported is $L_{max} = \lfloor C_{multi}/r \rfloor = \lfloor 30/6 \rfloor = 5$. If the average packet generation rate per link is $r = 3$ Mbps, then the maximum number of source-destination pairs that can be supported is $L_{max} = \lfloor C_{multi}/r \rfloor = \lfloor 30/3 \rfloor = 10$. When the number of source-destination pairs L is greater than L_{max} , packets will be dropped due to network saturation. Consequently, the packet failure rate and the average delay should increase dramatically.

Chapter 5

Simulation Results for Single-Hop WPAN Systems

In this chapter, the simulation results for single-hop WPAN based on the OFDM UWB physical layer are presented. The purpose behind using a single-hop scenario is to test the Physical and MAC layers developed in this study. Transmission systems for rates of 55 Mbps, 200 Mbps, and 480 Mbps are simulated in this study since they are representative of the lowest rate, the highest mandatory rate and the highest optional rate, respectively.

Both the 4m x 4m and the 10m x 10m geographic areas for the network regions are used for simulation studies of the single-hop scenarios. Since the transmission radii of MBOA OFDM UWB systems that achieve a PER of 8% are 12.0 m, 7.4 m, and 3.2 m for systems operating at 55 Mbps, 200 Mbps and 480 Mbps, respectively, the performance of the single-hop WPAN is easily estimated within these network areas. In addition to the average end-to-end delay and packet failure rate, the total throughputs for all source-destination pairs are also obtained.

Since the number of slots per frame is set to be the number of source-destination pairs, and each active source node is assigned one time slot within one frame, the packet loss due to collisions will be negligible. The scheduling efficiency should be close to 100%, theoretically. Generally, when the network saturation is reached, the packet failure rate will be increased dramatically due to the buffer overflow, and the average delay will also be increased due to extensive queueing.

Table 5.1 summarizes the system parameters used in the simulations for the single-hop scenarios considered in this study.

Simulation Parameter	Value
Simulation Time	10s
Number of Nodes	20
Number of Links	2, 4, 6, 8, 10
Network Area	4m × 4m, 10m × 10m
Number of Channels	1 (center frequency = 3.432 GHz)
Transmission Power	-10.3 dBm
Receiver Sensitivity	-77.2 dBm for 200 Mbps -72.6 dBm for 480 Mbps
Channel Models Considered	Free Space, Shadowing, and Rayleigh fading
Packet Size (application layer)	982 Bytes (will be 1024 Bytes after MAC layer)
Average Packet Generation Rate per Link	6 Mbps
Maximum Network Buffer Size	5,000 bytes
CTA Slot Duration	Transmission Duration of 1024-Byte Packet
Number of Slots per Frame	Number of Source-Destination Pairs (2, 4, 6, 8, 10)
Guard Time between Slots	1 μ s
Intra-Frame Time	1.875 μ s

Table 5.1: Simulation Parameters and Values for Single-Hop Scenarios.

5.1 4m × 4m Single-Hop System

The average delay, PFR, and throughput performance for the single-hop scenario within the 4m × 4m network area are illustrated in Figures 5.1 to 5.3 as a function of the number of source-destination pairs.

Since the source and destination nodes are randomly assigned, the average distance for the active links will be less than 3 m. It is recalled from Section 2.5 that the propagation ranges to achieve 8% PER for systems operating at 55 Mbps, 200 Mbps and 480 Mbps are about 12 m, 7.4 m, and 3.2 m, respectively. Therefore, if the physical layer and MAC layer developed in this study work well (that is, the system performance match those presented on the MBOA proposal, when considering the overheads of other network layers), the packet failure rate due to the channel error will be very small (close to zero) for transmission systems operating at 55 Mbps and 200 Mbps. However, there may be channel errors present for transmission systems operating at 480 Mbps.

For transmission systems operating at 55 Mbps, the saturation throughput, which is the achievable throughput when the network saturation occurs, is reached when 8 or more source-destination pairs are present. This is reasonable since the network throughput presented in [11] is about 48 Mbps at the physical layer for systems operating at 55 Mbps. It can be observed that the average delay is less than 5 ms, and the PFR is close to zero before the occurrence of throughput saturation. After saturation throughput (about 44 Mbps) has been reached, the average delay is increased to over 60 ms, and the PFR is increased to over 8%. It can be concluded that for single-hop scenarios within a 4m × 4m

area, the performance measures for average delay and PFR are both acceptable, and meet QoS requirements before the saturation of throughput is reached for transmission systems operating at 55 Mbps supporting real-time applications.

For transmission systems operating at both 200 Mbps and 480 Mbps, it can be observed that the network saturations are not reached even when 10 source-destination pairs are present. These results are reasonable since the network throughputs presented in [11] are about 120 Mbps and 180 Mbps for transmission systems operating at 200 Mbps and 480 Mbps. Both the average delay ($<5\text{ms}$) and PFR ($<5\%$) are small in this case. For systems operating at 480 Mbps, the PFR is slightly increased (from 0.072% to 1.38%) compared to that for the 200 Mbps transmission, however, it is still within the acceptable range ($<5\%$).

It has been verified that the simulation results for 4m x 4m single-hop scenarios match those presented in the MBOA OFDM UWB proposal, and the physical layer and MAC layer developed in this study function well for a 4m x 4m single-hop communication system configuration.

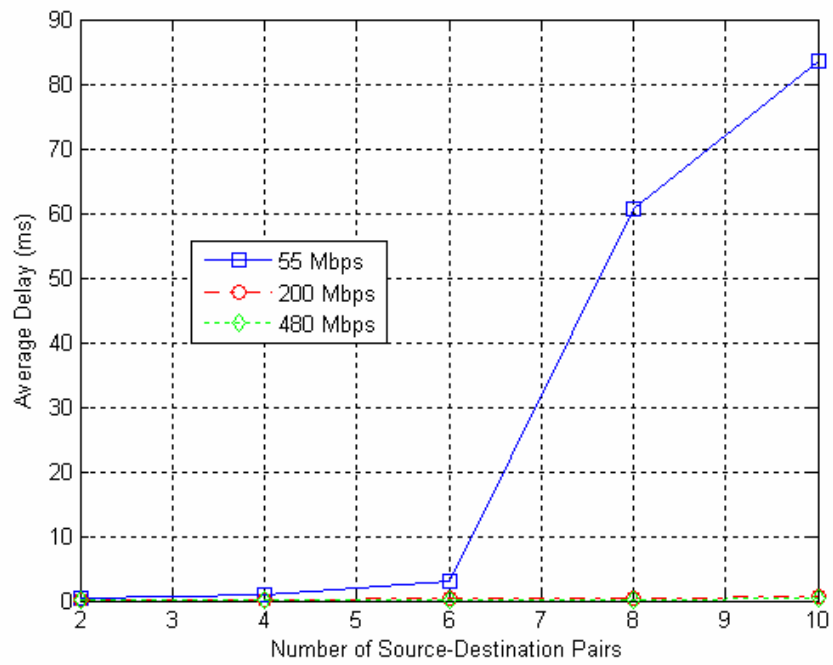


Figure 5.1: Average End-to-End Delay vs. Number of Source-Destination Pairs for Single-Hop Scenario: 4m x 4m Area.

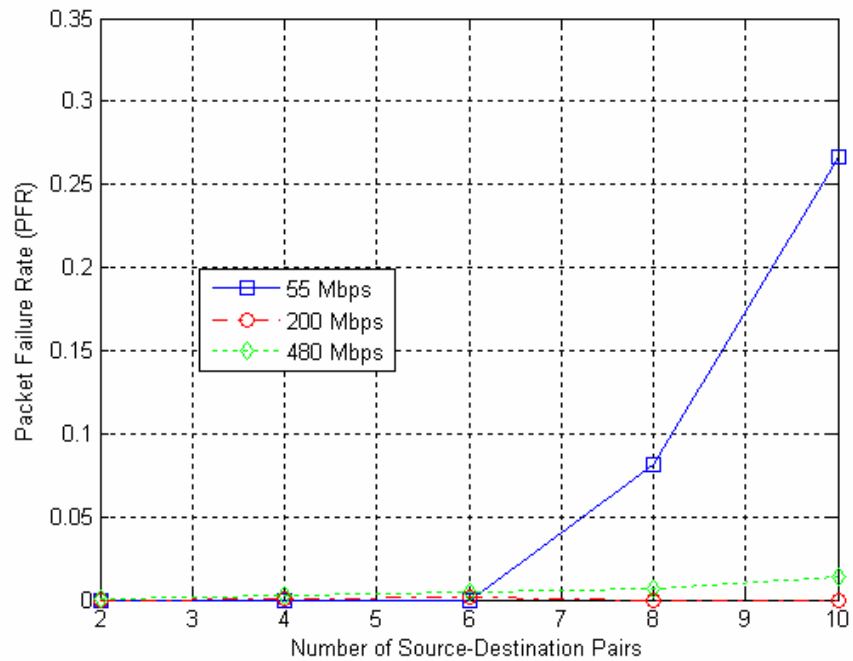


Figure 5.2: PFR vs. Number of Source-Destination Pairs for the Single-Hop Scenario: 4m x 4m Area.

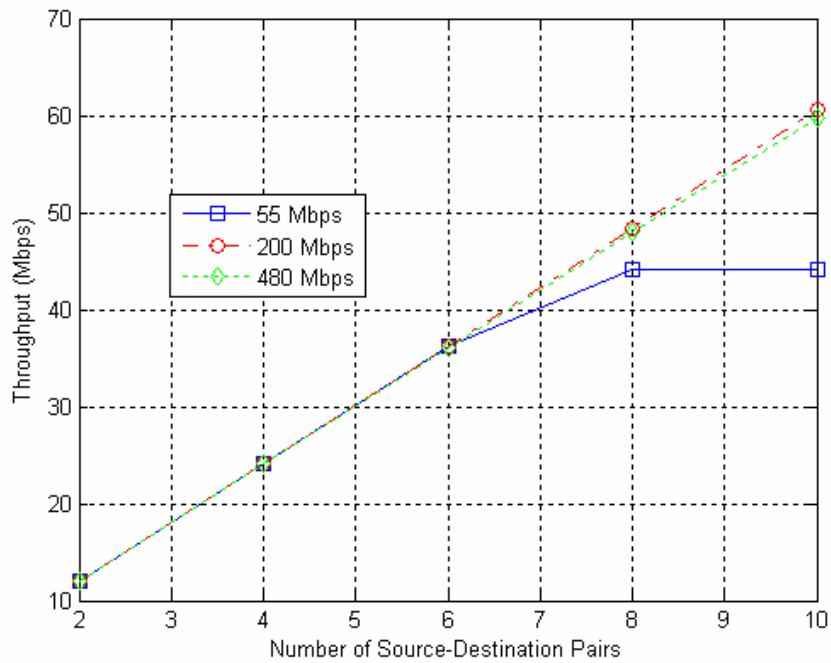


Figure 5.3: Throughput vs. Number of Source-Destination Pairs for Single-Hop Scenario: 4m x 4m Area.

5.2 10m x 10m Single-Hop System

The average delay, PFR, and throughput performance for the single-hop scenarios within a 10m x 10m area are illustrated in Figures 5.4 to 5.6 as a function of the number of source-destination pairs.

Since the source and destination nodes are randomly assigned, the average distance for the active links will be less than 7 m. Theoretically, if the physical layer and MAC layer developed in this study work well (that is, the system performances match those presented in the MBOA proposal, when considering the overheads of other network layers), the packet failure rate due to the channel error will be very small (close to zero) for the systems operating at 55 Mbps. However, there may be channel errors present for the systems operating at 200 Mbps. It is expected that there will be a large number of

channel errors present within those systems operating at 480 Mbps.

It can be observed that for systems operating at 55 Mbps, the performance is almost the same as that within the 4m x 4m area since it is still within the propagation range (about 12 m) in this case.

For systems operating at 200 Mbps, the saturation throughput is not reached even when 10 source-destination pairs are present. The average delay is very small, and less than 10 ms. The PFR is between 4% and 8%, which is much larger than the PFR obtained in the case of a 4m x 4m network area.

For systems operating at 480 Mbps, the saturation throughput is not reached even for 10 source-destination pairs. The average delay is very small, and less than 10 ms. However, the PFR is between 40% and 70%, which is much too large to be acceptable.

It can be seen that the achievable throughput for systems operating at 480 Mbps is much less than those for systems operating at 55 Mbps and 200 Mbps. This is because more packets are dropped due to the presence of higher channel BER.

It has been verified that the simulation results for 10m x 10m single-hop scenarios match those presented in MBOA OFDM UWB proposal, and the physical layer and MAC layer developed in this study perform well for a 10m x 10m single-hop communication system configuration.

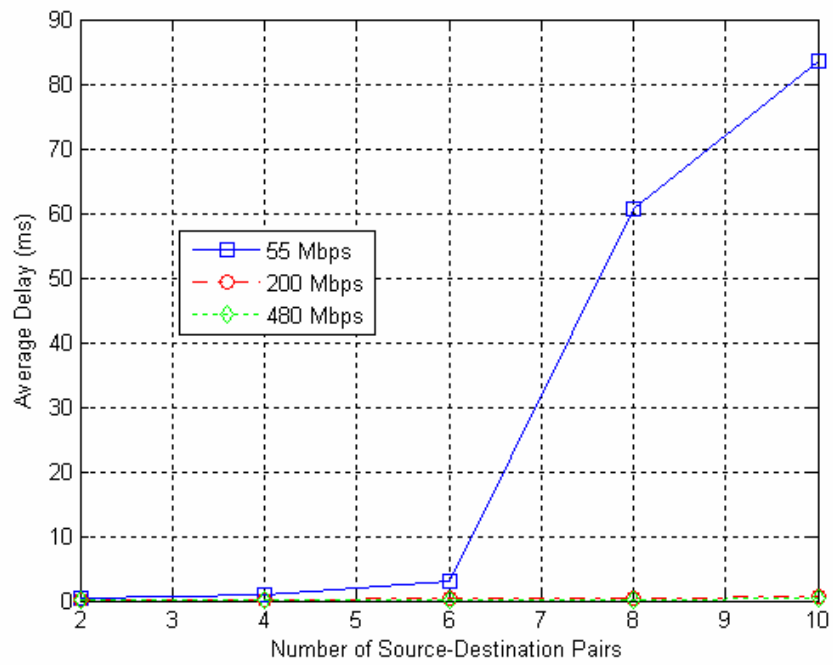


Figure 5.4: Average End-to-End Delay vs. Number of Source-Destination Pairs for Single-Hop Scenario: 10m x 10m Area.

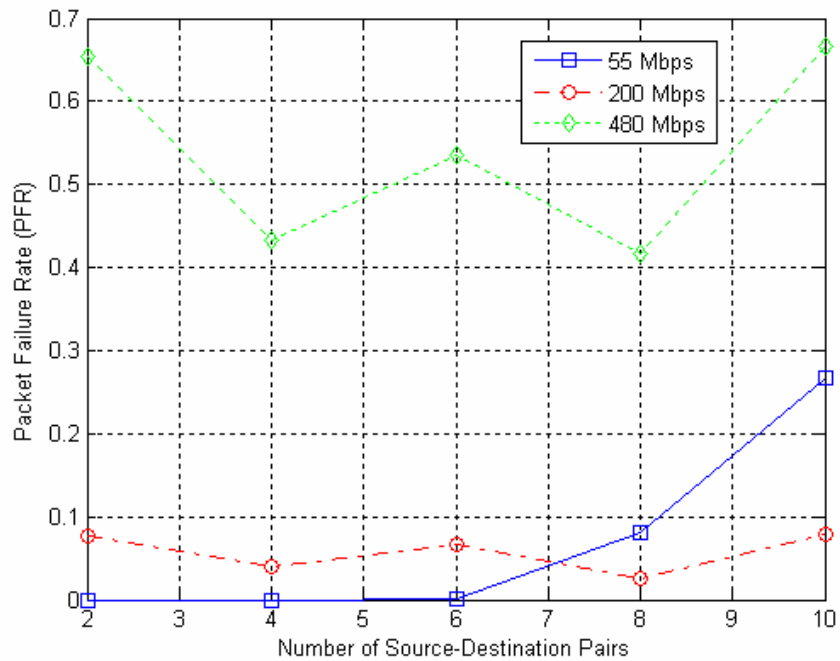


Figure 5.5: PFR vs. Number of Source-Destination Pairs for Single-Hop Scenario: 10m x 10m Area.

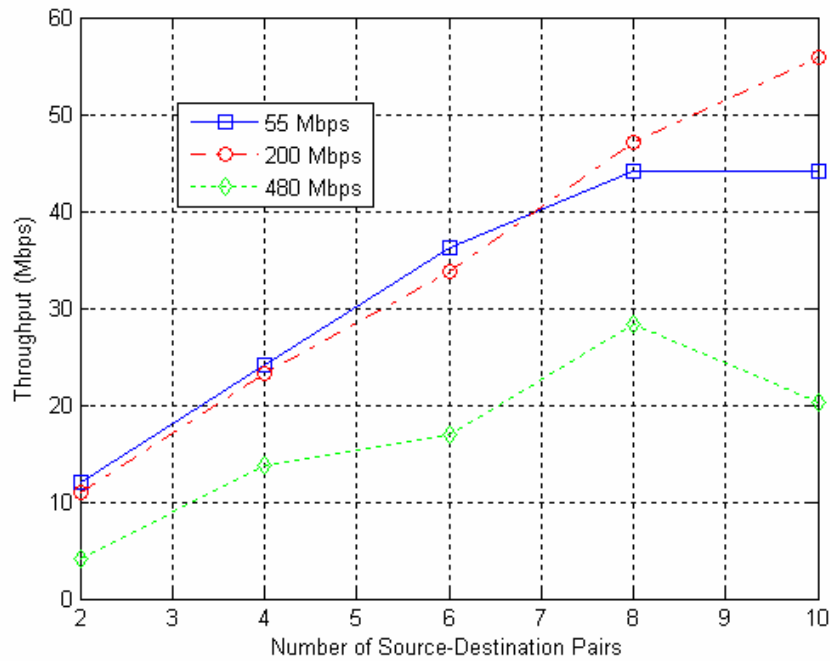


Figure 5.6: Throughput vs. Number of Source-Destination Pairs for Single-Hop Scenario: 10m x 10m Area.

5.3 Conclusions for Single-Hop Scenarios

Based on the results for both the 4m x 4m and 10m x 10m network areas, it can be observed that for single-hop WPAN systems, within the coverage radius, before the saturation throughput is reached, the performance criteria for all data rates (55, 200 and 480 Mbps), i.e. the average delay and PFR, meet the QoS requirements for real-time applications. It can also be concluded that the simulation results for single-hop scenarios match those presented in the MBOA OFDM UWB proposal. The physical layer and MAC layer developed in this study have been demonstrated to function well. Hence, the extension to the case of multi-hop communication system configurations will be developed next based on the physical layer and MAC layer implementations considered in this chapter.

Chapter 6

Routing Protocols Based on a Realistic Physical Layer

In a multi-hop ad hoc network, nodes communicate with each other using several wireless links. One of the important challenges in the design of multi-hop ad hoc networks is the development of routing protocols that can efficiently find routes between two communication nodes [6]. Hence, routing is a major issue that needs careful investigation in order to successfully transition from single-hop systems to multi-hop systems.

An ad hoc wireless network consists of a set of mobile nodes that are connected by wireless links. The network topology in such a network may keep changing in an almost random fashion. Routing protocols that find a path to be followed by data packets from a source node to a destination node used in traditional wired networks cannot be directly applied to the case of ad hoc wireless networks due to their highly dynamic topology, absence of an established infrastructure for centralized administration (e.g., base station or access points), bandwidth-constrained wireless links, and the presence of resource (energy)-constrained nodes [4]. A variety of routing protocols for ad hoc wireless networks have been proposed in recent years [4]. This chapter first presents the issues involved in designing a routing protocol, and then different classes of routing protocols are introduced briefly. The chapter then focuses on the design of routing protocols that are well suited for use in conjunction with a realistic physical layer. A position-based greedy stateless routing protocol is proposed for the multi-hop WPAN system employing

a realistic OFDM UWB physical layer wherein the signal strength fluctuations found in actual channel environments are considered. Finally, system simulation results are presented.

6.1 Issues in Designing a Routing Protocol

The major challenges encountered in the design of a routing protocol for ad hoc wireless networks include the mobility of nodes, resource constraints, error-prone channel state, and hidden and exposed terminal problems [4].

The network topology in an ad hoc wireless network is highly dynamic due to the movement of nodes. Hence, an on-going session may suffer from frequent path breaks. Disruption occurs either due to the movement of the intermediate nodes in the path, or due to the movement of end nodes. Therefore, wired network routing protocols cannot be used in ad hoc wireless networks wherein the mobility of nodes results in frequently changing network topologies. Routing protocols for ad hoc wireless networks must be able to perform efficient and effective mobility management as well [4].

Abundant bandwidth is available in wired networks due to the advent of fiber optics and the recent exploitation of wavelength division multiplexing technologies. But in a wireless communications network, the available radio spectrum is limited, and hence, the data rates that can be supported are much less than what a wired network can support. This requires that the routing protocols make use of the available bandwidth optimally by keeping the overhead as low as possible [4].

The broadcast nature of the radio channel poses a unique challenge for ad hoc wireless networks. The wireless links have time-varying characteristics in terms of both link capacity and link-error probability. This requires that the ad hoc wireless network routing protocols interact with the MAC layer to find alternative routings that use better-quality links. Also, the transmissions in ad hoc wireless networks often result in collisions of data and control packets [4]. If a TDMA MAC layer is used, the collision will be eliminated by the allocation of time slots, but the packets will be dropped due to the buffer overflow when congestion of the network occurs. Therefore, it is required that ad hoc wireless routing protocols find paths with less congestion [4].

Due to the issues associated with an ad hoc wireless network environment discussed so far, ad hoc wireless networks require specialized routing protocols that address the challenges described above [4].

6.2 Existing Routing Protocols

Dozens of routing protocols have been proposed for MANETs (Mobile Ad-Hoc Networks). These routing protocols for wireless ad hoc networks can be classified into different types based on specific criteria. The classification is not mutually exclusive and some protocols fall into more than one class. The routing protocols for ad hoc wireless networks can be broadly classified based on their routing information update mechanism, use of temporal information for routing, routing topology, and utilization of specific resources. In this section, we give a brief discussion of proactive routing protocols, reactive routing protocols, and geographic routing protocols.

In table-driven or proactive routing protocols, every node maintains the network topology information in the form of routing tables by periodically exchanging routing information. Routing information is generally flooded onto the entire network. Whenever a node requires a path to a destination, an appropriate path-finding algorithm is executed at the node using the local topology information that it maintains [4]. These protocols are extensions of the wired network routing protocols. They maintain the global topology information in the form of tables at every node. These tables are updated frequently in order to maintain consistent and accurate network state information. The destination sequenced distance-vector routing protocol (DSDV), wireless routing protocol (WRP), and source-tree adaptive routing protocol (STAR) are some examples of protocols that belong to this category [4].

The most popular routing protocols for wireless ad hoc networks are reactive, or on-demand routing protocols, such as AODV and DSR. Reactive protocols do not maintain the network topology information. They obtain the necessary path when it is required, by using a connection establishment process. Hence, these protocols do not exchange routing information periodically. Unlike the table-driven routing protocols, on-demand routing protocols execute the path-finding process and exchange routing information only when a path is required by a node to communicate with a destination [4].

There are also other ad hoc routing protocols that are based on the utilization of specific resources, such as power-aware routing and geographical information assisted routing, for example. For power-aware routing, the routing decisions are based on minimizing the

power consumption either locally or globally in the network [4]. Geographical information assisted routing protocols improve the performance of routing and reduce the control overhead by effectively utilizing the geographical information available [4]. These special purpose routing protocols are very useful in some specific situations.

6.3 Routing Protocols Based on a Realistic Physical Layer

Designers of most existing network layer protocols for ad hoc and sensor networks typically rely on the Unit Disk Graph (UDG) communication model, where two nodes communicate if, and only if, they are within distance R , where all nodes are assumed to have the same transmission radius. Almost all works reported in the literature use R as the independent variable in simulations of system behavior. While the protocols at the network layer are designed with simple assumptions and performance metrics, experiments are normally carried out using simulators that implement more realistic physical and Medium Access Control (MAC) layers [16].

Realistic network simulation tools often do not use the UDG model because it ignores random variations in received signal strengths that occur over time, which is typical in real-world applications. It was demonstrated that signal strength fluctuations have a significant impact on ad hoc network performance, sometimes more adversely affecting performance compared to node mobility. Thus, non-deterministic radio fluctuations cannot be ignored when designing robust ad hoc network protocols based on ad hoc network simulation and analysis [16].

Assuming a fixed signal-to-noise ratio (SNR), Figure 6.1 shows how the packet reception probability $p(x)$ depends on the distance x between two nodes within the network area. The exact shape of the curve depends on the exact communication model that is used. It is obvious that the UDG model is indeed a good initial approximation for this, since the reception probability is close to either 0 or 1 everywhere except around the edge of the transmission radius. Generally, it is hard to determine the exact value of the transmission radius R in Figure 6.1. Is $R = 30$? If so, then the failure rate for transmission is ≤ 5 percent. Is $R = 50$? If so, then the reception probability is ≥ 5 percent. Is $R = 41$? If so, then the packet reception rate is 0.5 [16]. When the transmission radius takes on different values of the distance x , the corresponding packet reception probability varies from 0 to 1. Hence, the link quality varies substantially.

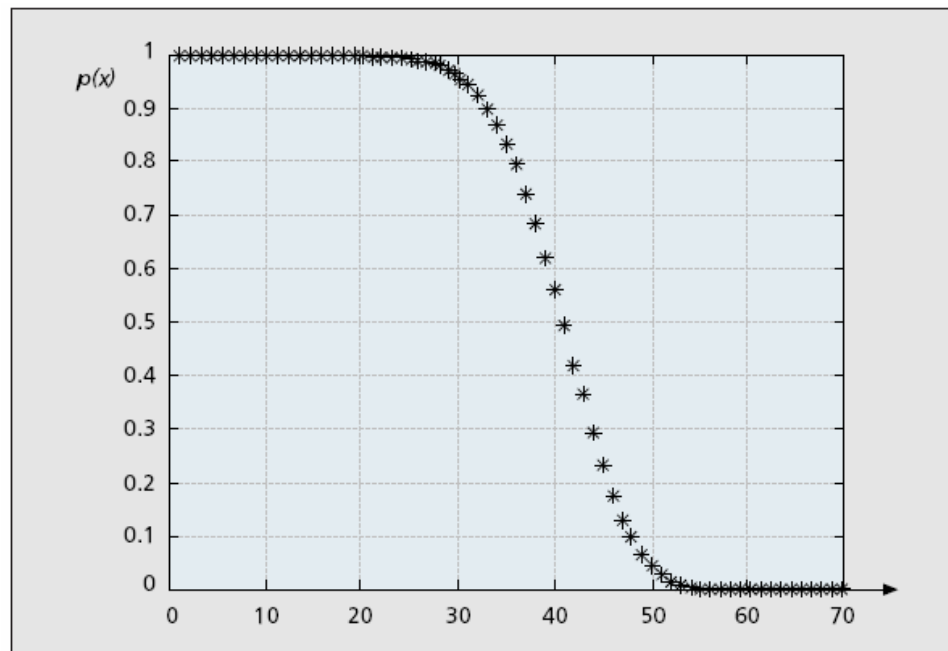


Figure 6.1: Packet Reception Probability as a Function of Distance in a Typical Physical Layer Model [16].

We can also use packet error rate (PER) as an indicator of the link quality, instead of the packet reception probability. With a realistic physical layer, the PER can be expressed as a function of distance x , $PER = p(x)$. For the MBOA OFDM UWB physical layer, Figure 6.2 shows how PER depends on the distance x between two nodes for systems operating at both 200 Mbps and 480 Mbps for the case of 1K-byte packets. For systems operating at 200 Mbps, when $x = 7$ m, PER is about 3%, and good link quality is provided. When $x = 9$ m, PER is about 95%, which results in a very poor link quality being realized.

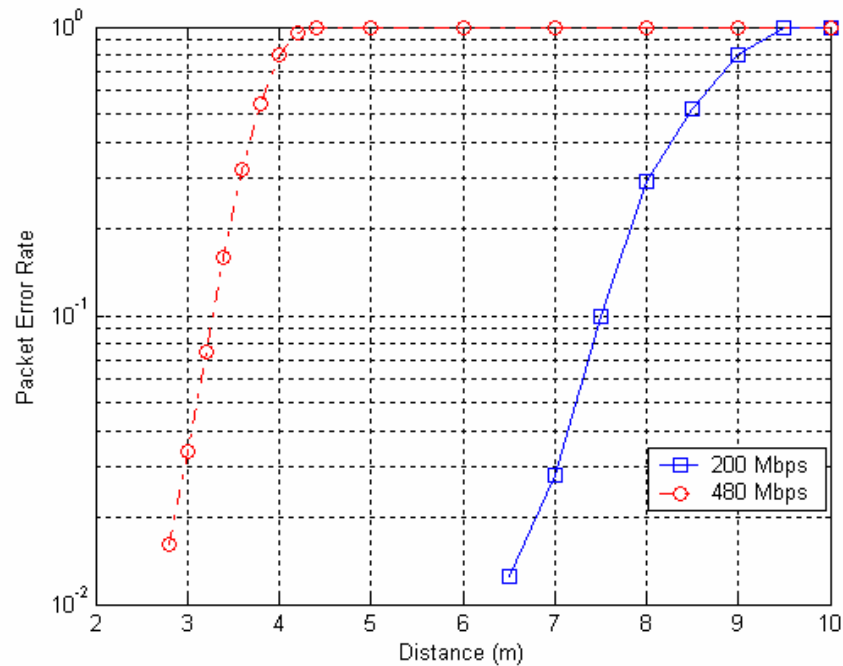


Figure 6.2: PER vs. Distance for the Proposed OFDM UWB Physical Layer [6].

As mentioned before, almost all of the existing protocols are designed based on a simplistic and idealistic physical layer model, in which signal strength fluctuations due to a realistic channel are not considered. Without modification, they cannot perform well in conjunction with a realistic physical layer. Much of the recent work in ad hoc routing

protocols for wireless networks has focused on coping with mobile nodes, rapidly changing topologies, and scalability. Less attention has been paid to finding high-quality paths in the face of lossy wireless links [18]. The metric most commonly used by existing ad hoc routing protocols is that of minimum hop-count. These protocols typically only use links that deliver routing probe packets (query packets, as in DSR or AODV, or routing updates, as in DSDV). This approach implicitly assumes that links will either work well, or not work at all. While often true in wired networks, this is not a reasonable approximation in the case of wireless networks: many wireless links have intermediate loss ratios. A link that delivers only 50% of the transmitted packets may not be useful for data, but might deliver enough routing update, or query packets, so that the routing protocol may be able to effectively use the link anyway [18].

When minimum hop count is used as the only metric for route selection, minimizing the hop-count maximizes the distance traveled by each hop, which is likely to minimize signal strength and maximize the loss ratio. Even if the best route is a minimum hop-count route, in a dense network there may be many routes of the same minimum length, with widely varying qualities. Hence, the arbitrary choice that is made by most minimum hop-count metrics is not likely to select the best route [18].

To solve this problem, link quality aware routing protocols (such as link aware Dynamic Source Routing or Ad-hoc On-Demand Distance Vector routing) could be considered for general ad hoc and sensor networks. That is, in addition to minimum hop count, link quality is also used as a route selection metric in the route discovery process. This

approach should be applicable to, and practical for, all ad hoc and sensor networks. For WPAN, since it is primarily used for home networking, most of the nodes will be stationary, and there are no frequent topology updates. Therefore, position-based routing should be a viable approach. Since the value of transmission radius R is changed with the threshold value of PER, it is closely related to the link quality. The value of transmission radius R then affects the performance significantly, and can serve as the routing metric [17]. The position-based greedy routing protocol used in our simulations is discussed in detail in the next section.

6.4 Position-Based Greedy Stateless Routing

In our study, a position-based routing protocol employing a greedy forwarding scheme is proposed for multi-hop WPANs based on a realistic OFDM UWB physical layer. The transmission radius R is assumed to be the distance where $PER = p(R)$ is equal to a preset threshold value (for example, 5%). We define two nodes as being neighbors if they are within R . Since the value of R is changed with the threshold value of PER, it is closely related to the link quality. It then affects the performance significantly, and can serve quite well as the routing metric. In this study, different values of R will be selected according to different PER levels, and the optimal value is obtained by trading off the packet failure rate (PFR) and throughput of multi-hop WPANs.

Position-based (or geographic) routing uses location information for packet delivery in multi-hop wireless networks. Neighbors locally exchange location information obtained either via the Global Positioning System (GPS) or some other location determination technique [21]. Since nodes locally select next hop nodes based on this neighborhood

information and the destination location, neither route establishment, nor per-destination state is required in position-based routing [21]. The properties for position-based routing, such as its stateless nature and low maintenance overhead, make it increasingly more attractive [21][22].

Stateless routing schemes are localized schemes where nodes do not need to memorize past traffic. All decisions are based on the location of neighboring nodes, location of the destination, the position of the neighboring node that forwarded the message in the previous step, and the information that arrives with the message. Hence, position-based localized algorithms avoid the overhead by requiring only accurate neighborhood information and the position of the destination. Here, the routing overhead is defined as the average number of routing protocol control packets that are present in the network.

For the position-based routing scheme implemented in this study, during the 30-second initialization period, the position information of all nodes will be obtained. Each node will keep a table to store the position information and calculate the distances from its neighbors. Since position-based routing is a localized algorithm, when a node needs to send a packet, it makes a decision as to which neighbor to forward the message based solely on the location of this node itself, its neighboring nodes, and the destination.

Since WPANs are widely used for home networks, most of the nodes will be stationary. Hence, in this study, all nodes will be kept stationary during the course of system simulation. Generally the link quality, which is quantitatively measured by PER, will

remain relatively stable when there is no node mobility. Therefore, we will focus on the route discovery process, and not pay much attention to the route maintenance process.

The most popular route discovery strategy for geographic routing is the greedy routing scheme based on Euclidean distance. The nodes holding the message simply forward data packets to the neighbor geographically closest to the destination [21][22]. As indicated in Figure 6.3, node S, currently holding the message, is aware only about the positions of its neighbors within the transmission radius R and the destination T. How R is selected will greatly affect the system performance. If R is chosen to be the maximum distance reachable, then A is closest to the destination T among all of the neighbors of S. This generally will lead to the least number of hop counts. However, the PER for the link between S and A is very high. Very bad link quality will be provided in this case. If R is chosen to be the distance where $PER = p(R) = 0.5$, packets will be forwarded to C. In this case, the link quality between C and A is not the best, but within an acceptable range. If R is chosen to be the distance where $PER = p(R) = 0.1$, B will be the next hop, and the link quality between A and B is very good. However, if R is chosen to be too small, the number of hops will be increased significantly. Then we may trade off the hop counts and link quality, and choose C for the next hop, and R for which $1\% < PER = p(R) < 5\%$ will be the optimum transmission radius [17].

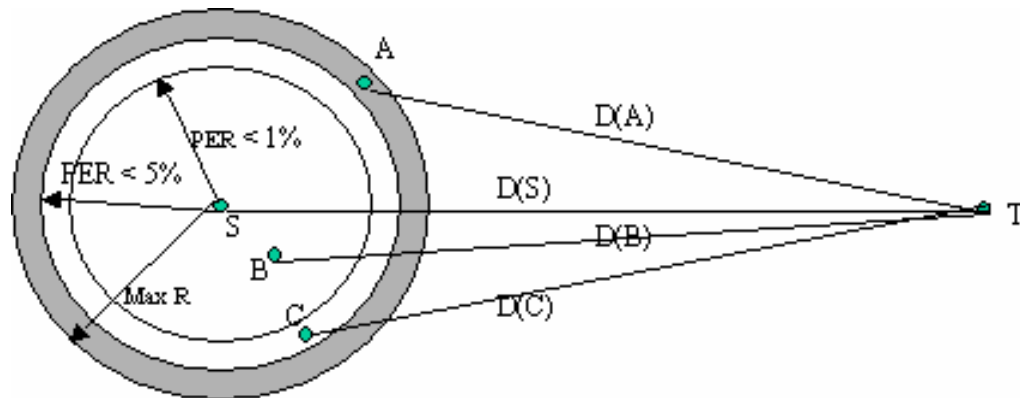


Figure 6.3: Illustration of Position-Based Routing [17].

6.5 Simulation Results

Transmission systems operating at both 200 and 480 Mbps have been simulated in this study. These systems were chosen since they are representative of the highest mandatory rate and the highest optional rate, respectively. The relevant parameters and their values used in the system simulations are listed in Table 6.1.

The network geographic area is set to be $20\text{m} \times 20\text{m}$ for systems operating at 200 Mbps, and $9\text{m} \times 9\text{m}$ for systems operating at 480 Mbps, which corresponds to different coverage radii (7.4 m and 3.2 m to achieve a PER of 8%, respectively). The area is limited such that the majority of the source-to-destination transmissions can take place with the number of hops less than the preset limit of 4, and the node density is sufficient for the position-based greedy routing scheme to work well.

Simulation Parameter	Value
Simulation Time	5s
Number of Nodes	20
Node's coverage radius to achieve PER of 8%	7.4m for 200 Mbps; 3.2m for 480 Mbps
Network Area	20m × 20m for 200 Mbps 9m × 9m for 480 Mbps
Number of Channels	1 (center frequency = 3.432 GHz)
Transmission Power	-10.3 dBm
Receiver Sensitivity	-77.2 dBm for 200 Mbps -72.6 dBm for 480 Mbps
Channel Model Considered	Free Space, Shadowing, and Rayleigh fading
Packet Size (application layer)	982 Bytes (will be 1024 Bytes after MAC layer)
Average Packet Generation Rate per Link	6 Mbps
CTA Slot Duration	Transmission duration of 1024-Byte Packet
Number of Slots per Frame	20 for 200 Mbps transmission 30 for 480 Mbps transmission

Table 6.1: Parameters and Values Used in System Simulations.

On-demand link-based scheduling is implemented for the TDMA MAC layer in the simulations. The number of slots per frame is fixed to be 20 for a transmission system operating at 200 Mbps, and 30 for a transmission system operating at 480 Mbps. The mean packet generation rate for each active link is 6 Mbps, which reflects the highest throughput requirement that is typically encountered in real-time VBR applications.

6.5.1 Simulation Results for Transmission Systems Operating at 200 Mbps

The network system simulations are performed by varying the transmission radius R . Figures 6.4 and 6.5 show the average delay and PFR with R as a parameter for

transmission systems operating at 200 Mbps. The average number of hops with different R for transmission systems at 200 Mbps are listed in Table 6.2.

The achievable throughput for peer-to-peer transmissions at 200 Mbps is about 120 Mbps as shown in [11]. For $R = 7.4$ m (the transmission radius needed to achieve a PER of 8%), the average hop count is 2.5. The network capacity C_{multi} shall be around $120/2.5 = 48$ Mbps, which means that a maximum of 8 links can be supported. It can be observed that when the link number $L < 8$, the PFR is approximately 10%, which is reasonable when the packet losses for intermediate nodes are considered. Both the average delay and the PFR increase dramatically when $L > 8$.

For $R = 6.9$ m (the transmission radius needed to achieve a PER of about 3%), the average hop count is 3.1, which leads to less network capacity. The network saturation is reached when there are more than 6 active links. However, both PFR ($< 7\%$) and average delay (< 40 ms) are acceptable for real-time applications before the occurrence of network saturation. It can also be observed that the PFR is larger than 10% when $R > 7.4$ m. Hence, the optimum value of R is approximately 6.9 m for transmission systems operating at 200 Mbps, which corresponds to a value of PER between 1% and 5%.

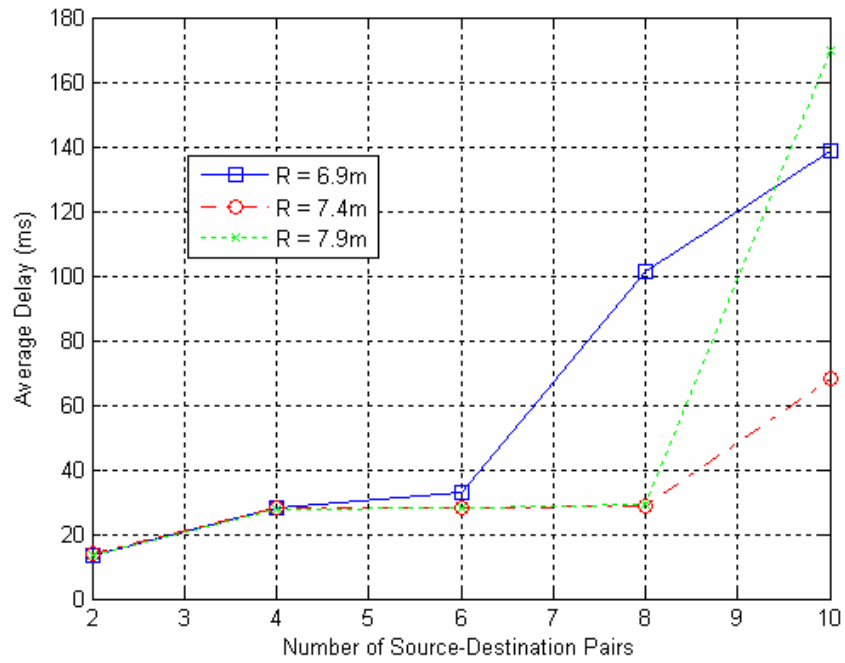


Figure 6.4: Average Delay vs. Number of Source-Destination Pairs With R as a Parameter for Transmission Systems Operating at 200 Mbps.

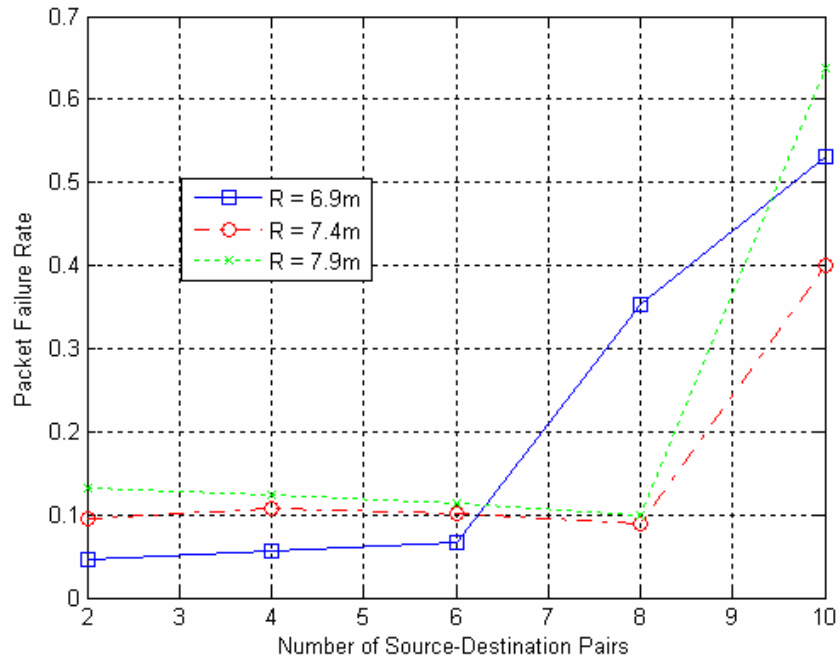


Figure 6.5: PFR vs. Number of Source-Destination Pairs With R as a Parameter for Transmission Systems Operating at 200 Mbps.

Transmission Radius R (m)	Average Hop Count
6.9	3.1
7.4	2.5
7.9	2.4

Table 6.2: Average Hop Count for Transmission Systems Operating at 200 Mbps.

6.5.2 Simulation Results for Transmission Systems Operating at 480 Mbps

The network system simulations are performed by varying the transmission radius R . Figures 6.6 and 6.7 illustrate the behavior of the performance measures for systems operating at 480 Mbps having R as a parameter. The average hop counts obtained for different values of R are listed in Table 6.3.

The achievable throughput for 480 Mbps peer-to-peer transmissions is approximately 180 Mbps as shown in [11]. When $R \geq 3.2$ m (the transmission radius needed to achieve a PER of 8%), the average hop count is $h \leq 2.9$, then $C_{multi} = 180/2.9 \cong 62$ Mbps, which means that at least 10 links can be supported. It can be observed that network saturation is not reached even when 10 active links are present when $R = 3.2$ m and $R = 3.45$ m. However, the PFR is greater than 8%, which is not acceptable for real-time applications.

For $R = 2.95$ m (the transmission radius needed to achieve a PER of 3%), the average hop count is 3.6, then $C_{multi} = 180/3.6 = 50$ Mbps, which means that at least $\lfloor 50/6 \rfloor = 8$ active links can be supported, theoretically. It can be observed that both the PFR (<7%) and the

average delay (<40ms) are acceptable for real-time applications before network saturation, although only 8 active links are supported. Hence, the optimum value of R for transmission systems operating at 480 Mbps is approximately 2.95 m, which corresponds to a value of PER between 1% and 5%.

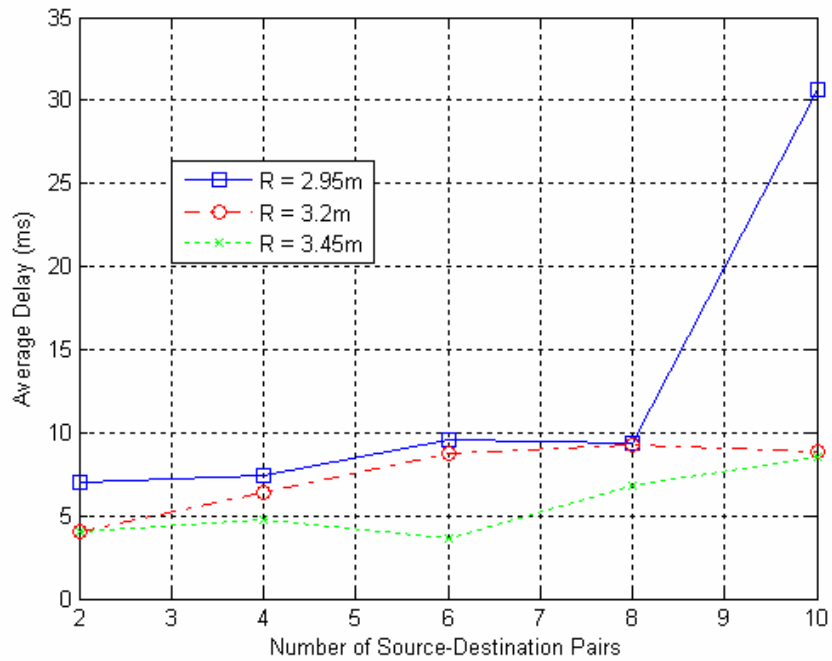


Figure 6.6: Average Delay vs. Number of Source-Destination Pairs with R as a Parameter for Transmission Systems Operating at 480 Mbps.

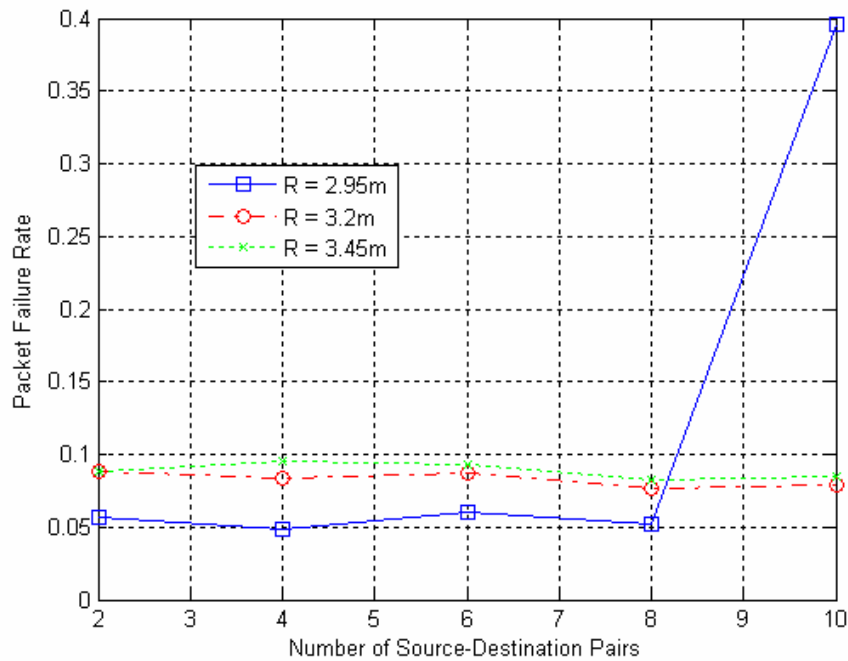


Figure 6.7: PFR vs. Number of Source-Destination Pairs with R as a Parameter for Transmission Systems Operating at 480 Mbps.

Transmission Radius R (m)	Average Hop Count
2.95	3.6
3.2	2.9
3.45	2.5

Table 6.3: Average Hop Count for Transmission Systems Operating at 480 Mbps.

6.5.3 Conclusions

One of the important observations obtained from the above results is that when R decreases, the PFR decreases due to the presence of fewer packet errors. However, decreasing R will cause the average hop count to be increased, which will lead to reduced throughput for multi-hop networks. The optimum value of R is selected to be the distance

required to achieve a value of PER between 1% and 5% by trading off the throughput efficiency and the PFR performance. This observation matches the theoretical analysis presented in Section 6.4.1.

In the ideal network environment, hop count is a valid metric for selecting routes. But in the context of a realistic physical layer, the shortest path often corresponds to the case of a high probability that two nodes are located on the edge of their useful transmission ranges [20]. For multi-hop WPANs based on an OFDM UWB physical layer, the position-based greedy routing scheme with carefully selected transmission radius R works well, and is a good choice for the routing protocol to be used in such networks.

Chapter 7

Simulation Results for Multi-Hop WPAN Systems

In this chapter, the simulation results for multi-hop communication system configurations are presented, and the associated performance analyses are given. Once again, transmission systems operating at 200 Mbps and 480 Mbps are simulated in this study since they are representative of the highest mandatory rate and the highest optional rate, respectively. First, the simulation results and performance analysis for the equal-weighted node-based scheduling scheme are presented. Then, the simulation results and performance analysis for the on-demand link-based scheduling scheme are presented. Finally, several conclusions are drawn for multi-hop WPAN systems operating in conjunction with a realistic OFDM physical layer.

7.1 System Parameters for Multi-Hop Scenarios

The network geographic coverage area is set to be $20\text{m} \times 20\text{m}$ for systems operating at 200 Mbps, and $9\text{m} \times 9\text{m}$ for systems operating at 480 Mbps, which corresponds to the different coverage radii (6.9 m and 2.95 m needed to achieve a PER of 5%, respectively). As has already discussed, a larger area results in the need for more hops, which in turn contributes to unfavorable delay accumulations. The network geographic area is limited such that the majority of the desired source-to-destination transmissions can take place with the number of hops being less than the preset limit of 4, and the node density is sufficient for the position-based greedy routing scheme to work well.

In Section 6.4, a position-based routing protocol with greedy forwarding scheme was proposed for multi-hop WPANs based on a realistic OFDM UWB physical layer. The simulation results described in Chapter 6 indicated that this position-based greedy routing scheme with carefully selected transmission radius R performs well for multi-hop WPANs based on a realistic OFDM UWB physical layer. This position-based routing scheme with $R = 6.9$ m for systems operating at 200 Mbps and $R = 2.95$ m for systems operating at 480 Mbps is employed in this study. Table 7.1 summarizes the system parameters used in the simulations for the multi-hop scenarios considered herein.

For systems operating at 200 Mbps, the achievable throughput for peer-to-peer transmission is approximately 120 Mbps [11]. It is known from Section 4.5 that for $R = 6.9$ m, the average hop count h is 3.1. The network capacity C_{multi} is on the order of $120/3.1 \cong 38$ Mbps theoretically, which means that a maximum of $\lfloor 38/6 \rfloor = 6$ links can be supported for a packet generation rate (PGR) equal to 6 Mbps per link. Furthermore, a maximum of $\lfloor 38/3 \rfloor = 12$ links can be supported when the PGR is equal to 3 Mbps per link. If the PGR is 128 kbps, the number of active links that can be supported will be approximately $\lfloor 38/0.128 \rfloor = 296$, which means there is more than enough overall system capacity for a 20-node network in this case.

For systems operating at 480 Mbps, the achievable throughput for peer-to-peer transmission is approximately 180 Mbps [11]. It is known from Section 4.5 that for $R = 2.95$ m, the average hop count h is 3.6. The network capacity C_{multi} is then approximately $180/3.6 = 50$ Mbps theoretically. In this case, a maximum of $\lfloor 50/6 \rfloor = 8$ links can be

supported for a PGR equal to 6 Mbps per link. Furthermore, a maximum of $\lfloor 50/3 \rfloor = 16$ links can be supported for a PGR equal to 3 Mbps per link. If the PGR is 128 kbps, the number of active links that can be supported will be $\lfloor 50/0.128 \rfloor = 390$, which means that there is more than enough capacity for a 20-node network in this case as well.

The above calculations are based on the assumptions that the bandwidth losses due to scheduling efficiency and routing overhead are negligible. As we already know, the position-based routing protocol used here avoids excessive overhead, and consequently the bandwidth loss due to the routing overhead is considered to be negligible. Therefore, the scheduling efficiency will be the major influence regarding how much capacity can be actually supported. If the scheduling efficiency is high, the capacity that can be actually supported will be close, or equal, to that determined theoretically. If the scheduling efficiency is low, the capacity that is actually realized will be lower than that theoretically predicted. The scheduling scheme that has the higher efficiency will be the most viable approach for use in this system.

Simulation Parameter	Value
Simulation Time	5s
Number of Nodes	20
Number of Links	2, 4, 6, 8, 10
Node's coverage radius to achieve a PER of 5%	6.9m for 200 Mbps; 2.95m for 480 Mbps
Network Area	20m × 20m for 200 Mbps 9m × 9m for 480 Mbps
Number of Channels	1 (center frequency = 3.432 GHz)
Transmission Power	-10.3 dBm
Receiver Sensitivity	-77.2 dBm for 200 Mbps -72.6 dBm for 480 Mbps
Channel Models Considered	Free Space, Shadowing, and Rayleigh fading
Packet Size (application layer)	982 Bytes (will be 1024 Bytes after MAC layer)
Network Buffer Size	100,000 bytes
CTA Slot Duration	Transmission duration of 1024-Byte Packet
Number of Slots per Frame for Equal-Weighted Node-Based Scheduling	20
Number of Slots per Frame for On-Demand Link-Based Scheduling	20, 40 for 200 Mbps 30, 60 for 480 Mbps
Guard Time between Slots	1 μ s
Intra-Frame Time	1.875 μ s

Table 7.1: Simulation Parameters and Values for Multi-Hop Network Scenarios.

7.2 Simulation Results for Equal-Weighted Node-Based Scheduling

The equal-weighted node-based scheduling scheme is first employed. The packet generation rates are taken to be 128 kbps, 3 Mbps and 6 Mbps. Figures 7.1 and 7.2 illustrate the average delay and the PFR with PGR taken as a parameter using the equal-weighted scheduling scheme for systems operating at 200 Mbps. Figures 7.3 and 7.4 illustrate the average delay and the PFR with PGR taken as a parameter using the equal-

weighted scheduling scheme for systems operating at 480 Mbps.

For equal-weighted node-based scheduling, each node has the same share of the bandwidth regardless of whether it has a packet to send or not and independent of how many packets it needs to send. For the total number of network nodes set to 20, each node can have $120/20 = 6$ Mbps of network bandwidth available for systems operating at 200 Mbps, and $180/20 = 9$ Mbps of network bandwidth available for systems operating at 480 Mbps.

If the PGR per link is 6 Mbps, only 1, or possibly 1.5 traffic streams can be supported by one node in either case. So, if a node is a sending node for one traffic stream and a forwarding node for another traffic stream, there will be collisions, and some of the packets will be dropped. This situation happens very often, and sometimes there are several traffic streams that need to be transmitted by one node at the same time. Hence, the system may work well with high probability only when the number of source-destination pairs is very small. The simulation results show that the performance measures are acceptable only when there are no more than 2 active links when the PGR equals 6 Mbps for systems operating at either 200 Mbps, or 480 Mbps. When the number of source-destination pairs L is greater than 2, both the PFR and the average delay increase dramatically.

Similarly, if the PGR per link is 3 Mbps, only 2 or 3 traffic streams can be transmitted from one node at the same time in either case. The situation is better than that for a PGR

equal to 6 Mbps, but the capacity available for each node is still not enough. It can be observed that a maximum of 4 active links can be supported. When $L > 4$, both the PFR and the delay increase dramatically. The maximum numbers of source-destination pairs that can be supported are less than the theoretically predicted capacities that were presented in Section 7.1 for systems operating at either 200 Mbps, or 480 Mbps. The scheduling efficiency is low, and the system bandwidth is wasted.

For a PGR equal to 128 kbps, there are over 50 traffic streams that can be supported by any one node at the same time for systems operating at either 200 Mbps, or 480 Mbps. It can be observed that the PFR (<8%) and the delay (about 5ms) both meet the QoS requirements for real-time applications even for 10 active links when the PGR is 128 kbps.

It can be clearly seen that the achieved network capacities in practice for network systems operating at both 200 Mbps and 480 Mbps are less than the theoretical values for capacity that were presented before in this section when the equal-weighted node-based scheduling was used. That is because the scheduling efficiency is low, and the overall network bandwidth is not fully utilized. The equal-weighted scheduling scheme only works well when either the packet generation rate is low, or there is only a very small number of active links. However, a UWB-based WPAN system is designed for high-data rate multimedia traffic, and hence, QoS requirements have to be met. The simple equal-weighted node-based scheduling cannot perform well in this type of situation. For high data rate traffic, the on-demand scheduling scheme has to be considered.

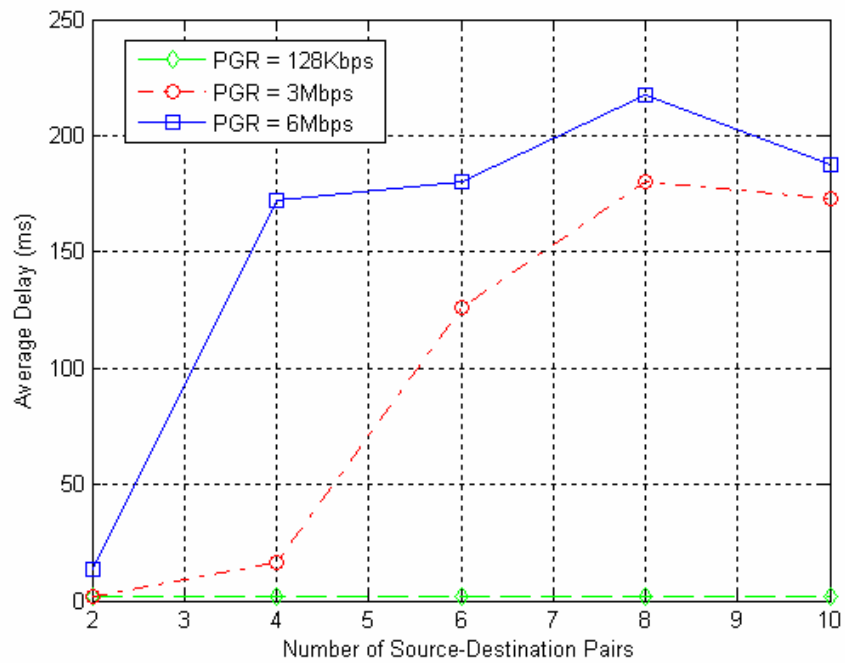


Figure 7.1: Average Delay vs. Number of Source-Destination Pairs With Equal-Weighted Scheduling for Transmission Systems Operating at 200 Mbps.

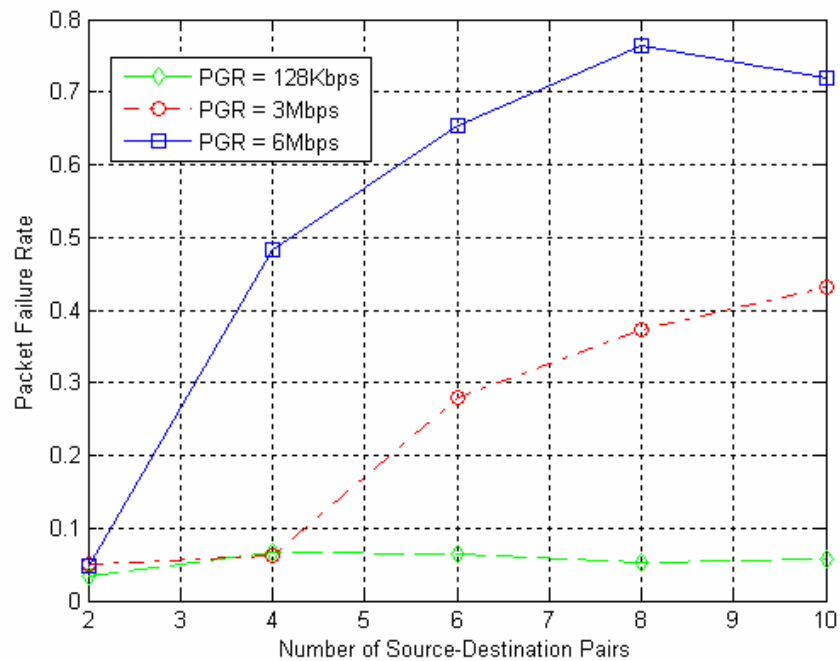


Figure 7.2: PFR vs. Number of Source-Destination Pairs With Equal-Weighted Scheduling for Transmission Systems Operating at 200 Mbps.

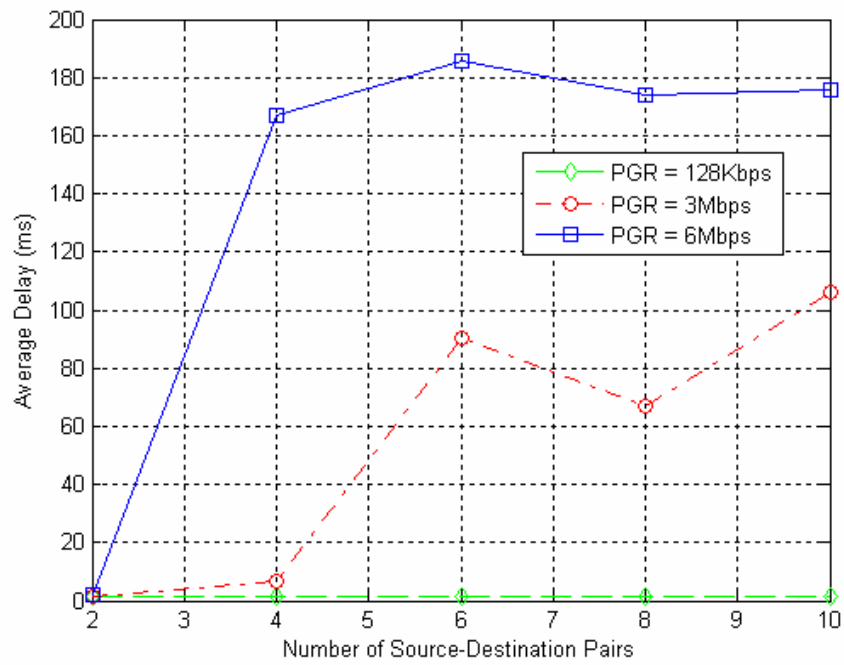


Figure 7.3: Average Delay vs. Number of Source-Destination Pairs With Equal-Weighted Scheduling for Transmission Systems Operating at 480 Mbps.

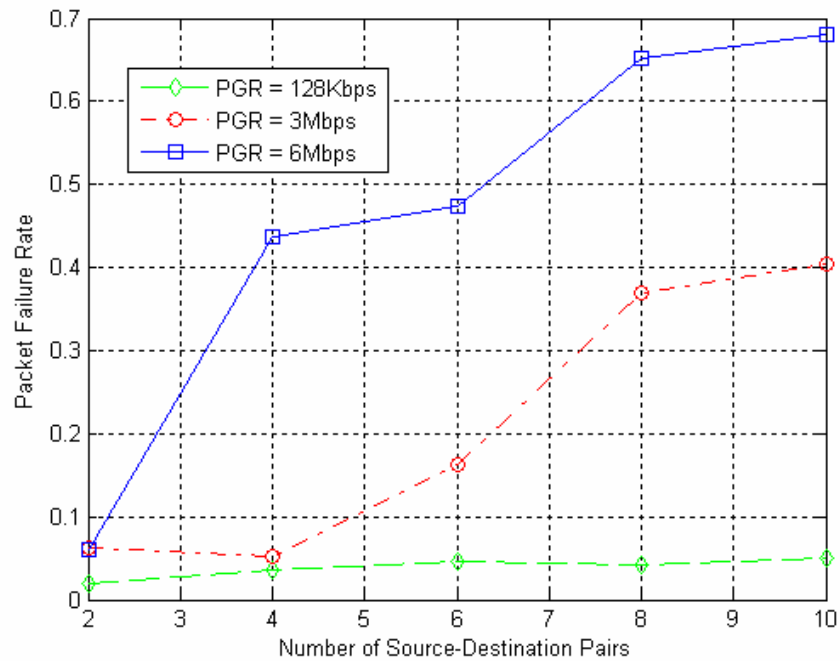


Figure 7.4: PFR vs. Number of Source-Destination Pairs With Equal-Weighted Scheduling for Transmission Systems Operating at 480 Mbps.

7.3 Simulation Results for On-Demand Link-Based Scheduling

For the on-demand link-based scheduling scheme, the packet generation rates are taken to be 3 Mbps and 6 Mbps. Given that the equal-weighted scheduling can work well for low data rates, a value for PGR of 128 Kbps is not considered here for the on-demand link-based scheduling scheme.

Figures 7.5 and 7.6 illustrate the average delay and the PFR with PGR, respectively, as a parameter using the on-demand link-based scheduling scheme for systems operating at 200 Mbps. It can be observed that saturation of the network is reached when there are more than 6 active links for a PGR equal to 6 Mbps. Both the PFR ($< 7\%$) and the delay (< 40 ms) are acceptable for real-time applications before network saturation occurs. Another observation is that both the PFR ($< 7\%$) and the delay (< 40 ms) are acceptable even for the case of 10 active links when the PGR is 3 Mbps per link. These simulation results for systems operating at 200 Mbps match the theoretically predicted capacities that were presented in Section 7.1. That is, a total of 6 links can be supported when the PGR is equal to 6 Mbps and 12 links can be supported when the PGR is equal to 3 Mbps.

Figures 7.7 and 7.8 illustrate the average delay and the PFR, respectively, using the on-demand scheduling scheme for systems operating at 480 Mbps. It can be observed that saturation of the network is reached when there are more than 8 active links for a PGR equal to 6 Mbps. Both the PFR ($< 7\%$) and the delay (< 10 ms) are acceptable before network saturation occurs. Another observation is that both the PFR ($< 7\%$) and the delay (< 10 ms) are acceptable even for the case of 10 active links when the PGR is 3

Mbps per link. The simulation results obtained for systems operating at 480 Mbps match the theoretically predicted capacities that were presented in Section 7.1. That is, 8 links can be supported when the PGR is equal to 6 Mbps and 16 links can be supported when the PGR is equal to 3 Mbps.

It can also be observed that both the PFR and the delay meet the QoS requirements for real-time applications even for 10 active links when the PGR is 3 Mbps per link. With the same network buffer size, the PFR is almost the same when the PGR is equal to 6 Mbps and when the PGR is equal to 3 Mbps. The delay when the PGR is equal to 3 Mbps is slightly smaller than that when the PGR is equal to 6 Mbps. This is reasonable since there will be more queueing delay associated with the higher data rate.

The simulation results described above for systems operating at both 200 Mbps and 480 Mbps match the capacity analysis for a multi-hop network given in Section 7.1. Therefore, it can be seen that the scheduling efficiency is comparatively higher for the on-demand scheduling scheme, and the network bandwidth can be utilized more efficiently than in the case of the equal-weighted scheduling scheme. It can be concluded that this UWB-based multi-hop WPAN system performs well when the on-demand link-based scheduling is employed along with the proper routing protocol.

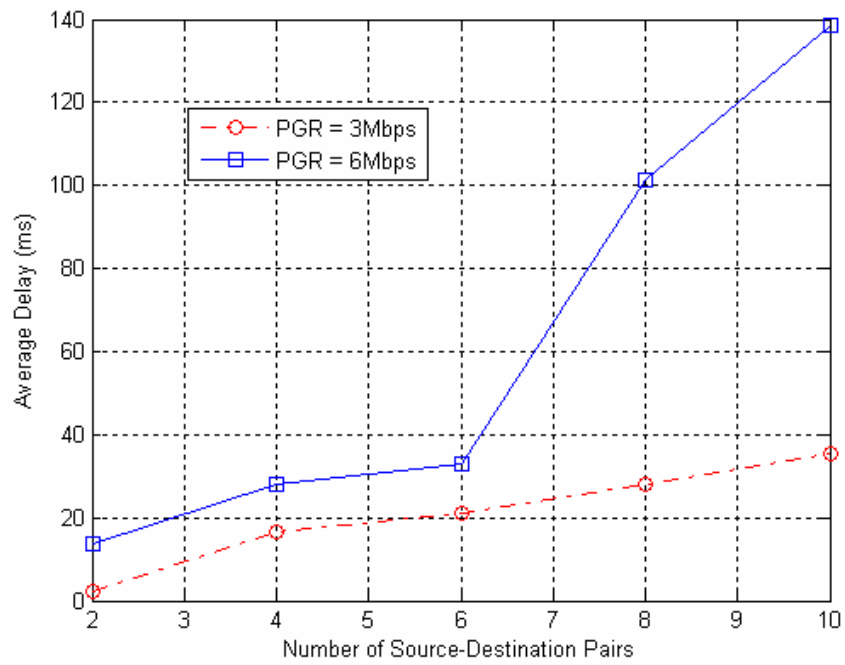


Figure 7.5: Average Delay vs. Number of Source-Destination Pairs With On-Demand Scheduling for Transmission Systems Operating at 200 Mbps.

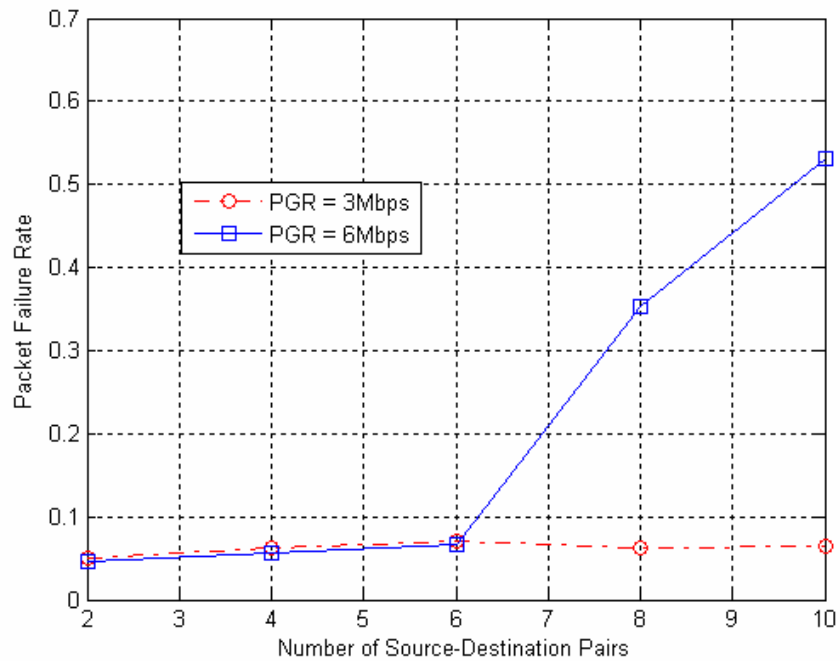


Figure 7.6: PFR vs. Number of Source-Destination Pairs With On-Demand Scheduling for Transmission Systems Operating at 200 Mbps.

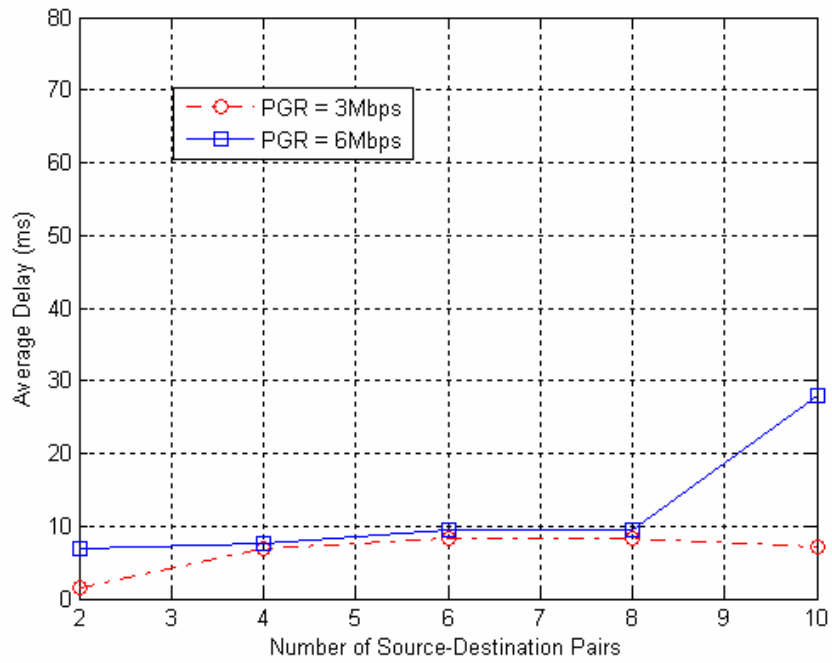


Figure 7.7: Average Delay vs. Number of Source-Destination Pairs With On-Demand Scheduling for Transmission Systems Operating at 480 Mbps.

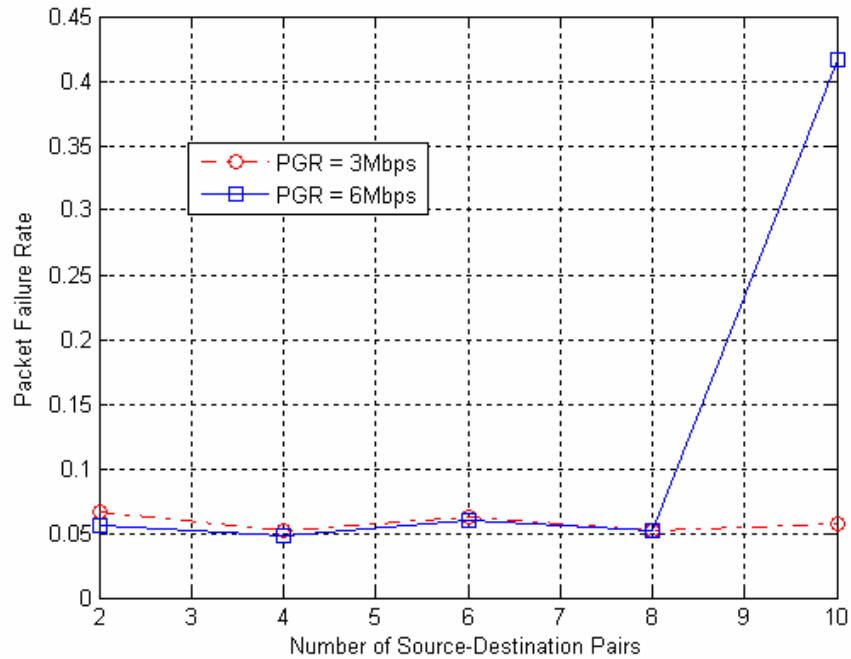


Figure 7.8: PFR vs. Number of Source-Destination Pairs With On-Demand Scheduling for Transmission Systems Operating at 480 Mbps.

7.4 Conclusions

Conclusions can be drawn based on the simulation results obtained and performance analyses described in the previous section.

The equal-weighted node-based scheduling scheme does not perform well for high-data rate applications. That is, the scheduling efficiency is low and much of the available network bandwidth had been wasted. This scheduling scheme only performs well when either the data rate is very low, or there are only a very small number of active links since the network bandwidth is not utilized efficiently.

The on-demand link-based scheduling scheme can perform well for the UWB-based multi-hop WPAN system considered here. That is, the scheduling efficiency is high, and the network bandwidth is utilized efficiently. Therefore, the IEEE 802.15.3 TDMA MAC layer with the proper scheduling and routing schemes function well in the context of multi-hop networks. Multi-hop WPANs based on a realistic OFDM UWB physical layer can be a viable approach to extend the network coverage while supporting very high data rate multimedia traffic.

Chapter 8

Conclusions and Future Work

In this dissertation, the feasibility regarding whether or not the IEEE 802.15.3 TDMA MAC layer can be effectively utilized in multi-hop WPANs based on the MBOA OFDM UWB physical layer has been explored through detailed and extensive system-level simulations. TDMA scheduling schemes and candidate routing schemes have been investigated. This chapter presents the main contributions of this research study. The overall research efforts and the related conclusions are introduced first. Next, several suggestions for future research directions are identified.

8.1 Contributions of the Thesis

In this study, complete WPAN transmission systems were implemented, including both single-hop and multi-hop network scenarios. A realistic OFDM UWB physical layer has been developed based on the MBOA OFDM UWB Proposal. Also a TDMA MAC layer has been developed based on the IEEE 802.15.3 Standard. At the network layer, a position-based greedy stateless routing protocol has been adopted in this study for use with multi-hop WPAN systems based on a realistic OFDM physical layer. At the MAC layer, both an on-demand link-based scheduling scheme and an equal-weighted node-based scheduling scheme have been implemented to determine their applicability for use in multi-hop WPAN scenarios. Simulation results and performance analysis are presented for single-hop scenarios, for position-based routing protocols, and for different scheduling schemes in multi-hop network scenarios.

The purpose of conducting simulations for single-hop network scenarios was to test and validate the UWB physical layer and MAC layer that had been developed in this study. It was observed that for single-hop WPAN systems, within the coverage radius and before the network saturation is reached, the selected performance criteria, i.e. the average delay and the PFR, meet the QoS requirements needed for real-time applications for all data rates (55, 200 and 480 Mbps). The simulation results for single-hop network scenarios match the performance levels described in the MBOA OFDM UWB Proposal. Furthermore, the results indicate that the physical layer and MAC layer developed in this research effort perform well.

A position-based stateless routing protocol with greedy forwarding was adopted in this study for multi-hop WPANs operating in conjunction with a realistic OFDM UWB physical layer. The transmission radius R is closely related to the link quality, and is defined by the achievable packet error rate (PER). The optimum value of R is selected to be that distance which achieves a value of PER between 1% and 5% by trading off the throughput and the packet failure rate (PFR). Simulation results show that the position-based stateless greedy routing scheme, with a carefully selected transmission radius R , can perform well. That is, the overall network system performance meets the QoS requirements for real-time applications before the occurrence of network saturation. Hence, this position-based stateless routing scheme with greedy forwarding would be a good choice for the routing protocol in multi-hop WPANs that utilize an OFDM UWB physical layer.

The simulation results for the TDMA MAC layer were presented subsequently. For the TDMA MAC layer, simulation results are presented for both an equal-weighted node-based scheduling algorithm and an on-demand link-based scheduling algorithm. When using equal-weighted topology-based scheduling, it can be clearly seen that the achievable network capacities for transmission systems operating at both 200 and 480 Mbps are much less than the capacity values that were predicted theoretically. The system performance can meet QoS requirements only when either the data rate is very low, or there are only a very small number of active links since the network bandwidth is not utilized efficiently. When using the on-demand rate-based scheduling, the performance results for transmission systems operating at both 200 and 480 Mbps match the capacity analyses results for multi-hop WPANs. The on-demand link-based scheduling scheme performs well for this UWB-based multi-hop WPAN system. That is, the scheduling efficiency is comparatively high, and hence, the network bandwidth can be utilized more efficiently.

It can be concluded that the IEEE 802.15.3 TDMA MAC layer, employing the proper scheduling and routing schemes, can function well. That is, the QoS requirements can be met in the case of multi-hop networks. Multi-hop WPAN systems based on an OFDM UWB physical layer can be a viable approach to extend the network coverage for very high data rate multimedia traffic.

We now revisit the example illustrated in Section 1.3. The network coverage problem encountered in the video conference or home theater application can be solved via the

implementation of multi-hop WPAN based on the OFDM UWB physical layer presented in this study. If a network area of 9m x 9m needs to be covered, a multi-hop WPAN system operating at 480 Mbps will support up to 8 traffic flows, with each flow operating at 6 Mbps. A system operating at 200 Mbps can even be used should lower data rates are required. If a network area of 20m x 20m needs to be covered, a multi-hop WPAN system operating at 200 Mbps will support up to 6 traffic flows, with each flow operating at 6 Mbps. In both cases, the QoS requirements can be met provided that the total traffic flows does not exceed the network capacity. For a video conference or a home theater system, support for 6 to 8 simultaneous traffic flows over a WPAN is sufficient.

8.2 Future Work

In cases where the topology and location information cannot be easily obtained, the modified on-demand wireless ad hoc routing schemes may be considered. Link quality, in conjunction with the hop count, should be used as the metric for route selection. Link quality aware on-demand routing protocols, such as DSR or AODV, could be good candidates for multi-hop WPANs based on the OFDM UWB physical layer.

Since WPAN is used for the networking of electronic devices within the home, most of the nodes will be stationary, and there are no frequent topology updates. Hence, the disadvantage of DSR could be minimized due to the limited mobility nature of WPAN. Therefore, it may be that DSR is a better approach than AODV in such a multi-hop WPAN system based on a UWB physical layer because it can save bandwidth by reducing the amount of overhead. In this approach, the route discovery process of the DSR routing protocol is modified to select a route based on both hop counts and the

packet delivery ratio of the link. Each node monitors and maintains the link quality statistics by measuring the packet delivery ratio from its immediate neighbors. During the route selection process, wireless links with a packet delivery ratio below a certain predetermined threshold are excluded so that the protocol only chooses a stable route. However, if there is no stable route available, then the weak links are reconsidered so that the overall network connectivity is preserved [19].

For the MAC layer, more efficient channel scheduling should be considered so as to increase overall network capacity. One candidate is S-TDMA, which should be investigated to see whether or not it will perform well in these scenarios. Spatial reuse TDMA, which is an extension of TDMA, is a collision-free access scheme for ad hoc networks. The basic idea is to let spatially separated radio terminals reuse the same time slot when the resulting interferences are not too severe. The capacity is thereby increased via the spatial reuse of the time slots, i.e., a time slot can be shared by radio units sufficiently separated geographically so that any residual interference is small.

For multi-hop WPAN systems based on a UWB physical layer, network capacity becomes the primary issue due to the short transmission range and the very high transmission rate that is typically required for multimedia traffic. Generally, the short transmission range increases the hop count from source to destination, and then leads to a reduction in the achievable network capacity for regular TDMA. Therefore, S-TDMA shall be a good alternative to that of regular TDMA for multi-hop WPAN systems since it can increase network capacity efficiently due to time slot reuse.

References

- [1] J. Karaoguz, "High-Rate Wireless Personal Area Networks," *IEEE Communications Magazine*, Vol. 39, pp. 96-102, December 2001.
- [2] S. M. S. Sadough, A. Mahmood, E. Jaffrot and P. Duhamel, "Performance Evaluation of IEEE 802.15.3a Physical Layer Proposal Based on Multiband-OFDM," <http://www.lss.superlec.fr/>.
- [3] R. Bruno, M. Conti and E. Gregori, "Mesh Networks: Commodity Multihop Ad Hoc Networks," *IEEE Communications Magazine*, pp. 123-131, March 2005.
- [4] C. S. Murthy and B. S. Manoj, *Ad Hoc Wireless Networks: Architecture and Protocols*, Prentice-Hall, NJ, 2004.
- [5] S. Xu and T. Saadawi, "Does the IEEE 802.11 MAC Protocol Work Well in Multihop Wireless Ad Hoc Networks?," *IEEE Communications Magazine*, pp. 130-137, June 2001.
- [6] F. Eshghi, A. K. Elhakeem and Y. R. Shayan, "Performance Evaluation of Multihop Ad Hoc WLANs," *IEEE Communications Magazine*, pp. 107-115, March 2005.
- [7] A. F. Molisch, J. R. Foerster and M. Pendergrass, "Channel Models for Ultrawideband Personal Area Network," *IEEE Wireless Communications Magazine*, Vol. 10, pp. 14-21, December 2003.
- [8] M. D. Benedetto and G. Giancola, *Understanding Ultra Wide Band Radio Fundamentals*, Prentice-Hall, NJ, 2004.
- [9] A. Saleh and R. Valenzuela, "A Statistical Model for Indoor Multipath Propagation," *IEEE Journal on Selected Areas in Communications*, Vol. 11, No. 7, pp. 967-978, September 1993.
- [10] L. Maret, I. Siaud and Y. Kamiya, "Ultra WideBand PHY Layer MBOA Performance and Sensitivity to Multipath Channels (IST Magnet Project)," <http://www.ist-magnet.org/>.
- [11] MultiBand OFDM Alliance, "Multi-Band OFDM Physical Layer Proposal for IEEE 802.15 Task Group 3a," September 14, 2004, <http://www.wimedia.org/>.
- [12] H. Xu and A. Ganz, "A Radio Resource Control Method in UWB Protocol Design," *Military Communications Conference*, Vol. 2, pp. 886-891, October 2003.

- [13] S. Datta, I. Seskar and M. Demirhan, "Ad-hoc Extensions to the 802.15.3 MAC Protocol," *Proceedings of the Sixth IEEE International Symposium on a World of Wireless Mobile and Multimedia Networks (WoWMoM'05)*, Taormina, Giardini Naxos, pp. 293-298, June 2005.
- [14] A. Rangnekar and K. Sivalingam, "Multiple Channel Scheduling in UWB Based IEEE 802.15.3 Networks," *Proceedings of the First International Conference on Broadband Networks (BROADNETs)*, San Jose, CA, pp. 406-415, October 2004.
- [15] H. Fattah and C. Leung, "An Overview of Scheduling Algorithms in Wireless Multimedia Networks," *IEEE Wireless Communications Magazine*, pp. 76-83, October 2002.
- [16] I. Stojmenovic, A. Nayak and J. Kuruvila, "Design Guidelines for Routing Protocols in Ad Hoc and Sensor Networks with a Realistic Physical Layer," *IEEE Communications Magazine*, pp. 101-106, March 2005.
- [17] H. Gao and D. G. Daut, "Position-Based Greedy Stateless Routing for Multihop WPANs Based on a Realistic UWB Physical Layer," *Second IEEE International Conference on Wireless Communications, Networking, and Mobile Computing (WiCOM)*, Wuhan, P. R. China, September 2006.
- [18] D. Couto, D. Aguayo, J. Bricket and R. Morris, "A High-Throughput Path Metric for Multi-Hop Wireless Routing," *International Conference on Mobile Computing and Networking (MobiCom)*, San Diego, CA, pp. 134-146, September 2003.
- [19] H. Tsai, N. Wisitpongphan and O. K. Tonguz, "Link-Quality Aware Ad Hoc On-Demand Distance Vector Routing Protocol," *First International Symposium on Wireless Pervasive Computing*, Phuket, Thailand, January 2006.
- [20] L. Qin and T. Kunz, "On-demand Routing in MANETs: The Impact of a Realistic Physical Layer Model," *Proc. Second International Conference on Ad Hoc, Mobile and Wireless Networks*, Montreal, Canada, pp. 37-48, October 2003.
- [21] S. Lee, B. Bhattacharjee and S. Banerjee, "Efficient Geographic Routing in Multihop Wireless Networks," *International Symposium on Mobile Ad Hoc Networking and Computing (MobiHoc)*, Urbana-Champaign, IL, pp. 230-241, May 2005.
- [22] I. Stojmenovic, "Position-Based Routing in Ad Hoc Networks," *IEEE Communications Magazine*, pp. 128-134, July 2002.
- [23] P. Mohapatra, J. Li and C. Gui, "QoS in Mobile Ad Hoc Networks," *IEEE Wireless Communications Magazine*, pp. 44-52, June 2003.

- [24] I. Stojmenovic, A. Nayak, J. Kuruvilla, F. Ovalle-Martinez and E. Villanueva-Pena, "Physical Layer Impact on the Design and Performance of Routing and Broadcasting Protocols in Ad Hoc and Sensor Networks," *Computer Communications*, Vol. 28, pp. 1138-1151, June 2005.
- [25] J. Gronkvist, "Distributed Scheduling for Mobile Ad Hoc Networks - A Novel Approach," *Fifteenth IEEE International Symposium on Personal, Indoor, and Mobile Radio Communications (PIMRC)*, Barcelona, Spain, Vol. 2, pp. 964-968, September 2004.
- [26] IEEE 802.15.3, "IEEE Standard 802.15.3: Wireless Medium Access Control (MAC) and Physical Layer (PHY) Specifications for High Rate Wireless Personal Area Networks (WPANs)," IEEE, Piscataway, NJ, September 2003.
- [27] Scalable Network Technologies (SNT), "Qualnet 3.8 Programmer's Guide," Version 1, <http://www.qualnet.com>.
- [28] D. Bertsekas and R. Gallager, *Data Networks*, Prentice-Hall, NJ, 1992.

Curriculum Vitae

Hongju Gao

- 9/1989 – 7/1993 Zhengzhou University, Zhengzhou, P. R. China.

Bachelor of Engineering in Detection Technology and Instrument, July 1993.
- 9/1997 – 1/2001 Rutgers, The State University of New Jersey, Department of Electrical and Computer Engineering, New Brunswick, New Jersey.

Master of Science in Electrical and Computer Engineering, January 2001.
- 7/2000 – 12/2002 Senior Network System Engineer, Engineering Department, Cingular Wireless (formerly Bellsouth Wireless Data), Woodbridge, New Jersey.
- 1/2003 – 5/2007 Rutgers, The State University of New Jersey, Department of Electrical and Computer Engineering, New Brunswick, New Jersey.

Doctor of Philosophy in Electrical and Computer Engineering, October 2007.